The Mathematics of Darwinian Systems

By

Peter Schuster*

Abstract: Optimization is studied as the interplay of selection, recombination and mutation. The underlying model is based on ordinary differential equations (ODEs), which are derived from chemical kinetics of reproduction, and hence it applies to sufficiently large – in principle infinite – populations. A flowreactor (*continuously stirred tank reactor*, CSTR) is used as an example of a realistic open system that is suitable for kinetic studies. The mathematical analysis is illustrated for the simple case of selection in the CSTR. In the following sections the kinetic equations are solved exactly for idealized conditions. A brief account on the influences of finite population size is given in the last section.

1 Replication in the flowreactor

Replication and degradation of molecular species $\mathbf{I}_i$ $(i = 1, 2, \ldots, n)$ in the flowreactor (figure 1) follows the mechanism

$$\begin{aligned} \star &\xrightarrow{a_0\, r} \mathbf{A} \\ \mathbf{A} + \mathbf{I}_i &\xrightarrow{k_i} 2\,\mathbf{I}_i \\ \mathbf{I}_i &\xrightarrow{d_i} \mathbf{B} \\ \mathbf{A}\,,\,\mathbf{B}\,,\,\mathbf{I}_i &\xrightarrow{r} \varnothing\ , \end{aligned} \tag{1}$$

and is described by the following $(n + 2)$ kinetic differential equations

$$\begin{aligned} \dot{a} &= -\Big(\sum_{j=1}^{n} k_i\, c_i\Big)\, a \;+\; r\,(a_0 - a)\ , \\ \dot{c}_i &= \Big(k_i\, a \;-\; (d_i + r)\Big)\, c_i\ ,\ \ i = 1, 2, \ldots, n \ \text{ and} \\ \dot{b} &= \sum_{j=1}^{n} d_j\, c_j \;-\; r\, b\ . \end{aligned} \tag{2}$$

The variables $a(t)$, $b(t)$, and $c_i(t)$ are molar concentrations, $[\mathbf{A}] = a$, $[\mathbf{B}] = b$, and $[\mathbf{I}_i] = c_i$, which are defined by $a = N_{\mathsf{A}}/(V\, N_A)$, $b = N_{\mathsf{B}}/(V\, N_A)$, and $c_i = N_i/(V\, N_A)$ where V is the volume and N_A is Avogadro's number, the

*Address: Institut für Theoretische Chemie der Universität Wien
Währingerstraße 17, A-1090 Wien, Austria
E-Mail: pks@tbi.univie.ac.at

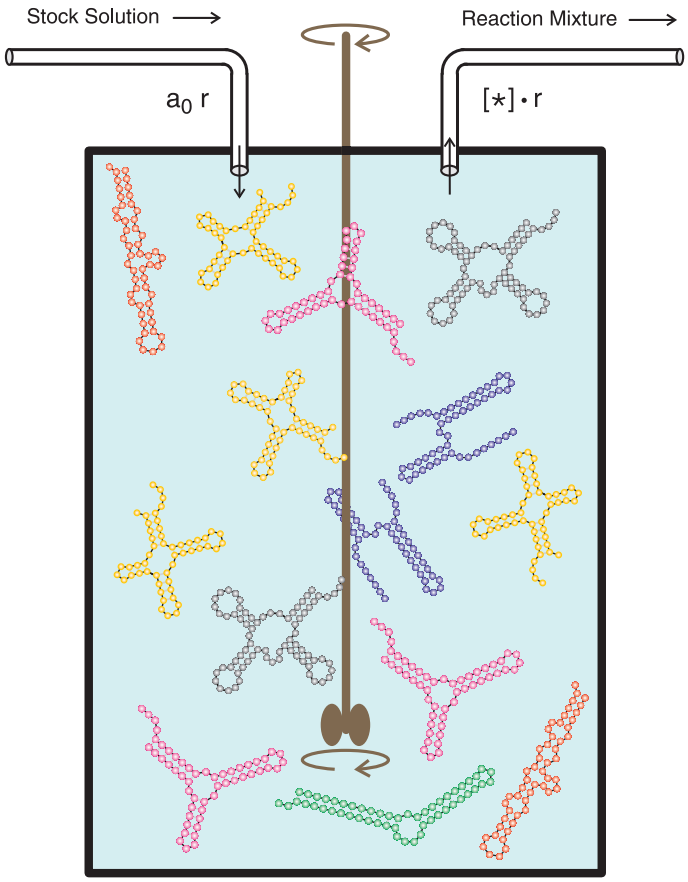

Figure 1: The flowreactor for the evolution of RNA molecules. A stock solution containing all materials for RNA replication ($[\mathbf{A}] = a_0$) including an RNA polymerase flows continuously at a flow rate r into a well stirred tank reactor (CSTR) and an equal volume containing a fraction of the reaction mixture ($[*] = \{a, b, c_i\}$) leaves the reactor (For different experimental setups see Watts [1]). The flow rate r has the dimension of a reciprocal time $[t^{-1}]$, and $\tau_r = r^{-1}$ represents the mean residence time of a volume element in the reactor. The population of RNA molecules ($\mathbf{I}_1, \mathbf{I}_2, \ldots, \mathbf{I}_n$ present in the numbers $N_1, N_2, \ldots, N_n$ with $N = \sum_{i=1}^{n} N_i$) in the reactor fluctuates around a mean value, $N \pm \sqrt{N}$. RNA molecules replicate and mutate in the reactor, and the fastest replicators are selected. The RNA flow reactor has been used also as an appropriate model for computer simulations [2–4]. There, other criteria for selection than fast replication can be applied. For example, fitness functions are defined that measure the distance to a predefined target structure and mean fitness increases during the approach towards the target [4].

number of particles in one mole substance. The particle numbers N are discrete and non-negative quantities, whereas concentrations are assumed to be continuous because $N_A = 6.023 \times 10^{23}\,\mathrm{mol}^{-1}$ is very large.[1]

The equations (2) sustain $(n+1)$ stationary states fulfilling the conditions $\dot{a} = 0, \dot{b} = 0, \dot{c}_i = 0$ for $i = 1, 2, \ldots, n$. Every stationarity conditions for one

[1] An overview of the notation used in this article is found on the last page.

particular class of replicating molecules $\mathbf{I}_i$

$$\bar{c}_i \left(k_i \, \bar{a} \; - \; (d_i + r) \right) \; = \; 0$$

has two solutions (i) $\bar{c}_i \; = \; 0$ and (ii) $\bar{a} \; = \; (d_i + r)/k_i$. Since any pair of type (ii) conditions is incompatible,[2] only two types of solutions remain: (i) $\bar{c}_i \; = \; 0 \; \forall \; i \; = \; 1, 2, \ldots, n$, the state of extinction, because no replicating molecule survives and (ii) n states with $\bar{c}_j \; = \; (a_0/(d_j + r) \; - \; 1/k_j) \, r$ and $\bar{c}_k \; = \; 0 \; \forall \; k \; \neq \; j$. Steady state analysis through linearization and diagonalization of the Jacobian matrix at the stationary points yields the result that only one of the n states is asymptotically stable, in particular the one for the species $\mathbf{I}_m$ that fulfils

$$k_m \, a_0 \; - \; d_m \; = \; \max\{a_j k_j - d_j \, , \; j = 1, 2, \ldots, n\} \; . \tag{3}$$

Accordingly, species $\mathbf{I}_m$ is selected and we call this state the state of selection. The proof is straightforward and yields simple expressions for the eigenvalues λ_k $(k = 0, 1, \ldots, n)$ of the Jacobian matrix when degradation is neglected, $d_j = 0$ $(j = 1, 2, \ldots, n)$. For the state of extinction we find

$$\lambda_0 \; = \; - \, r \;\; \text{and} \;\; \lambda_j \; = \; k_j \, a_0 \; - r \; . \tag{4}$$

It is asymptotically stable as long as $r > k_m \, a_0$ is fulfilled. If $r > k_m a_0$ then $r > k_j \, a_0 \; \forall \; j \neq m$ is valid by definition because of the selection criterion (3) for $d_j = 0$. For all other n pure states, $\{\bar{c}_i = a_0 - r/k_i \, , \; \bar{c}_j = 0 \, , \; j \neq i\}$ the eigenvalues of the Jacobian are:

$$\begin{aligned} \lambda_0 \; &= \; - \, r \; , \\ \lambda_i \; &= \; - \, k_i \, a_0 \; + \; r \; , \quad \text{and} \\ \lambda_j \; &= \; - \, \frac{r}{k_i} \; (k_j - k_i) \; \forall \; j \neq i. \end{aligned} \tag{5}$$

All pure states except the state at which $\mathbf{I}_m$ is selected (state of selection: $c_m = a_0 - r/k_m \, , \; c_j \; = \; 0 \, , \; j \; = \; 1, \ldots, n, j \; \neq \; m$) have at least one positive eigenvalue and are unstable. Therefore we observe indeed selection of the molecular species with the largest value of k_j (or $k_j \, a_0 - d_j$, respectively), because only at $\bar{c}_m \neq 0$ all eigenvalues of the Jacobian matrix are negative.

It is worth indicating that the dynamical system (2) has a stable manifold $\bar{y} = \bar{a} + \bar{b} + \sum_{i=1}^{n} \bar{c}_i = a_0$ since $\dot{y} = \dot{a} + \dot{b} + \sum_{i=1}^{n} \dot{c}_i = (a_0 - y) \, r$. The sum of all concentrations, $y(t)$, follows a simple exponential relaxation towards the steady state $\bar{y} = a_0$:

$$y(t) \; = \; a_0 \; - \left(a_0 - y(0) \right) \exp(-r \, t) \; ,$$

with the flow rate r being the relaxation constant.

[2]We do not consider degenerate or neutral cases, $d_i = d_j$ and $k_i = k_j$, here (see also section 7).

2 Selection

As shown in the previous section the basis of selection is reproduction in the form of a simple autocatalytic elementary step, $(\mathbf{A}) + \mathbf{I}_i \to 2\mathbf{I}_i$. We idealize the system by assuming that the material consumed in the reproduction process, $\mathbf{A}$, is present in excess. Therefore, its concentration is constant and can be subsumed as a factor in the rate constant: $f_i = k_i\,[\mathbf{A}]$. In addition we neglect the degradation terms by putting $d_i = 0\ \forall\ i$. In terms of chemical reaction kinetics selection based on reproduction without recombination and mutation is described by the dynamical system

$$\dot{c}_i \;=\; f_i\,c_i \;-\; \frac{c_i}{\sum_{j=1}^{n} c_j(t)}\,\Phi(t) \;=\; c_i\left(f_i - \frac{1}{c(t)}\,\Phi(t)\right)\ ,\ i = 1, 2, \ldots, n\ . \quad (6)$$

As before the variables $c_i(t)$ are the concentrations of the genotypes I_i, the quantities f_i are reproduction rate parameters corresponding to over-all replication rate constants in molecular systems or, in general, the fitness values of the genotypes. A global flux $\Phi(t)$ has been introduced in order to regulate the growth of the system. Transformation to relative concentrations, $x_i(t) = c_i(t)/c(t)$ with $c(t) = \sum_{j=1}^{n} c_i(t)$, and adjusting the global flux $\Phi(t)$ to zero net-growth yields:[3]

$$\begin{aligned} \dot{x}_i \;&=\; f_i\,x_i \;-\; x_i \sum_{j=1}^{n} f_j\,x_j \;=\; x_i(f_i - \Phi) \quad \text{with} \\ \Phi &= \frac{1}{c(t)} \sum_{j=1}^{n} f_j\,c_j(t) = \sum_{j=1}^{n} f_j\,x_j(t) = \overline{f} \quad \text{and} \quad i = 1, 2, \ldots, n\ . \end{aligned} \quad (7)$$

The relative concentrations $x_i(t)$ fulfil $\sum_{j=1}^{n} x_j(t) = 1$ and the flux $\Phi(t)$ is the mean growth rate of the population. Because of this conservation relation only $n-1$ variables x_i are independent. In the space of n Cartesian variables, $\mathbb{R}^n$, the x-variables represent a projection of the positive orthant onto the unit simplex (figure 2)

$$\mathbb{S}_n^{(1)} = \left\{ x_i \geq 0\,\forall\, i = 1, 2, \ldots, n\ \wedge\ \sum_{i=1}^{n} x_i = 1 \right\}\ .$$

The simplex $\mathbb{S}_n^{(1)}$ is an invariant manifold of the differential equation (7). This means that every solution curve $\mathbf{x}(t) = \big(x_1(t), x_2(t), \ldots, x_n(t)\big)$ that starts in one point of the simplex will stay on the simplex forever.

[3]Care is needed for the application of relative coordinates, because the total concentration $c(t)$ might vanish and then relative coordinates become spurious quantities (see subsection 6.7).

In order to analyze the stability of $\mathbb{S}_n^{(1)}$ we relax the conservation relation $\sum_{i=1}^n x_i(t) = c(t)$ and assume that only the conditions

$$\{f_i > 0 \wedge 0 \leq x_i(0) < \infty\} \forall\, i = 1, 2, \ldots, n \ ,$$

are fulfilled. According to this assumption all rate parameters are strictly positive – a condition that will be replaced by the weaker one $f_i \geq 0 \forall\, i \neq k \wedge f_k > 0$ – and the concentration variables are non-negative quantities. Stability of the simplex requires that all solution curves converge to the unit simplex from every initial condition, $\lim_{t\to\infty}\left(\sum_{i=1}^n x_i(t)\right) = 1$.
This conjecture is proved readily: From $\sum_{i=1}^n x_i(t) = c(t)$ follows

$$\dot{c} \ = \ c\left(1 - \frac{c}{c^0}\right) \Phi(t) \ = \ c\,(1-c)\,\Phi(t) \text{ with } \ \Phi(t) \ > \ 0 \ , \tag{8}$$

and $c^0 = 1\,M$ being the unit concentration. For $\dot{c} = 0$ we find the two stationary states: a saddle point at $\bar{c} = 0$ and an asymptotically stable state at $\bar{c} = 1$. There are several possibilities to verify its asymptotic stability, we choose to solve the differential equation and find:

$$c(t) \ = \ \frac{c(0)}{c(0) + \big(1 - c(0)\big)\, \exp\left(-\int_0^t \Phi(\tau) d\tau\right)} \, .$$

Starting with any positive initial value $c(0)$ the population approaches the unit simplex. When it starts on $\mathbb{S}_n$ it stays there even in presence of fluctuations.[4] Therefore, we restrict population dynamics to the simplex without loosing generality and characterize the state of a population at time t by the vector $\mathbf{x}(t)$ which fulfils the $\mathbb{L}^{(1)}$ norm $\sum_{i=1}^n x_i(t) = 1$.

The necessary and sufficient condition for the stability of the simplex, $\Phi(t) > 0$, enables us to relax the condition for the rate parameters f_i. In order to have a positive flux it is sufficient that one rate parameter is strictly positive provided the corresponding variable is non-zero:

$$\Phi(t) \ > \ 0 \implies \exists k \in \{1, 2, \ldots, n\} \text{ such that } f_k > 0 \wedge x_k > 0 \ .$$

For the variable x_k it is sufficient that $x_k(0) > 0$ holds because $x_k(t) \geq x_k(0)$ when all other products $f_j x_j$ were zero at $t = 0$. This relaxed condition for the flux is important for the handling of lethal mutants with $f_j = 0$.

[4] Generalization to arbitrary but finite population sizes $c \neq 1$ is straightforward: For $\sum_{i=1}^n x_i(0) = c_0$ the equation $\dot{x_i} \ = \ f_i x_i \ - \ (x_i/c_0) \sum_{j=1}^n f_j x_j$, $i = 1, 2, \ldots, n$ plays the same role as equation (7) did for $\sum_{i=1}^n x_i(0) = 1$.

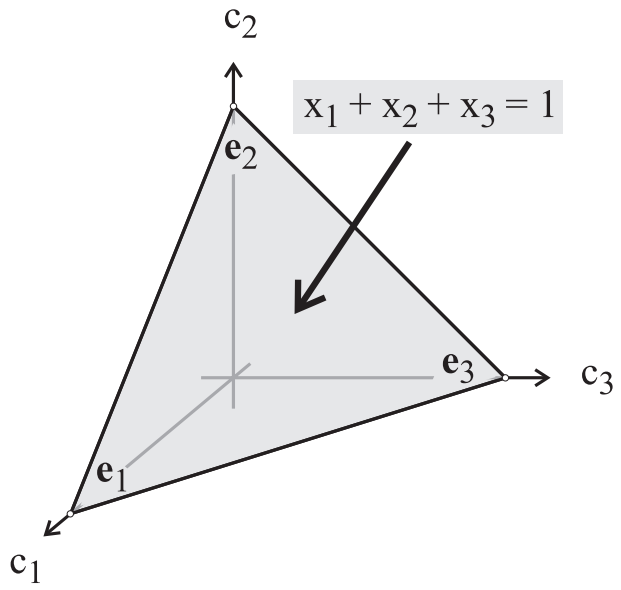

Figure 2: The unit simplex. Shown is the case of three variables (c_1, c_2, c_3) in Cartesian space $\mathbb{R}^{(3)}$ projected onto the simplex $\mathbb{S}_3^{(1)}$. The condition $x_1+x_2+x_3 = 1$ defines an equilateral triangle in $\mathbb{R}^{(3)}$ with the three unit vectors, $\mathbf{e}_1 = (1, 0, 0)$, $\mathbf{e}_2 = (0, 1, 0)$, and $\mathbf{e}_3 = (0, 0, 1)$ as corners.

The time dependence of the mean fitness or flux Φ is given by

$$\begin{aligned}\frac{d\Phi}{dt} &= \sum_{i=1}^{n} f_i \dot{x}_i = \sum_{i=1}^{n} f_i \left(f_i x_i - x_i \sum_{j=1}^{n} f_j x_j \right) = \\ &= \sum_{i=1}^{n} f_i^2 x_i - \sum_{i=1}^{n} f_i x_i \sum_{j=1}^{n} f_j x_j = \\ &= \overline{f^2} - \left(\overline{f}\right)^2 = \mathrm{var}\{f\} \geq 0 \, . \end{aligned} \tag{9}$$

Since a variance is always nonnegative, equation (9) implies that $\Phi(t)$ is a non-decreasing function of time. The value $\mathrm{var}\{f\} = 0$ refers to a homogeneous population of the fittest variant, and then $\Phi(t)$ cannot increase any further. Hence it has been optimized during selection.

It is also possible to derive analytical solutions for equation (7) by a transform called integrating factors ([5], p.322ff.):

$$z_i(t) = x_i(t) \exp\left(\int_0^t \Phi(\tau) d\tau \right) \, . \tag{10}$$

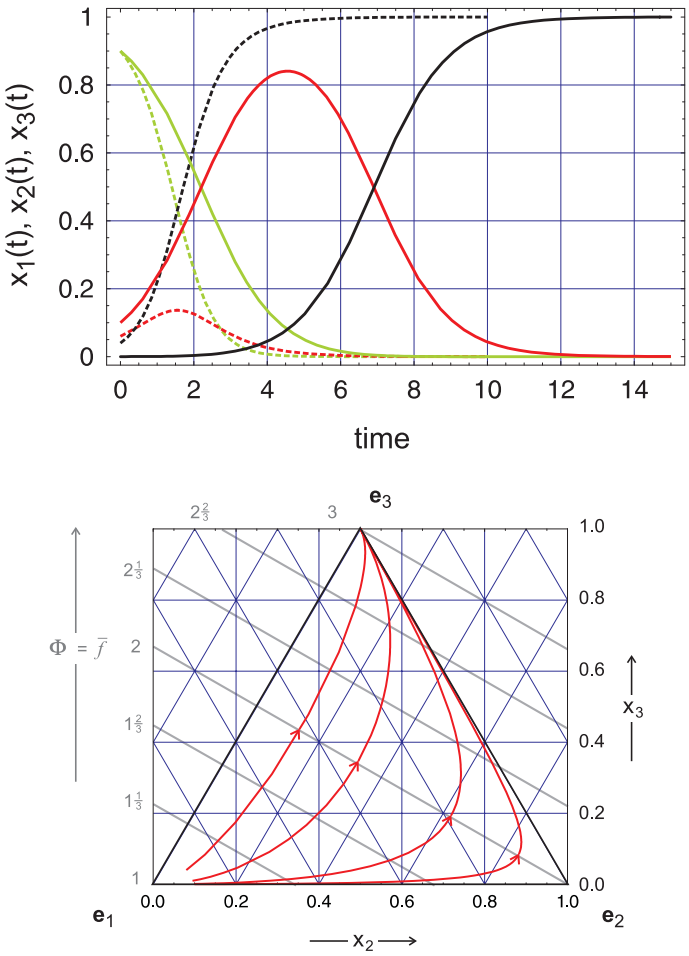

Figure 3: Selection on the unit simplex. In the upper part of the figure we show solution curves $\mathbf{x}(t)$ of equation (7) with $n = 3$. The parameter values are: $f_1 = 1\,[\mathrm{t}^{-1}]$, $f_2 = 2\,[\mathrm{t}^{-1}]$, and $f_3 = 3\,[\mathrm{t}^{-1}]$, where $[\mathrm{t}^{-1}]$ is an arbitrary reciprocal time unit. The two sets of curves differ with respect to the initial conditions: (i) $\mathbf{x}(0) = (0.90, 0.08, 0.02)$, dotted curves, and (ii) $\mathbf{x}(0) = (0.9000, 0.0999, 0.0001)$, full curves. Color code: $x_1(t)$ green, $x_2(t)$ red, and $x_3(t)$ black. The lower part of the figure shows parametric plots $\mathbf{x}(t)$ on the simplex $\mathbb{S}_3^{(1)}$. Constant level sets of Φ are straight lines (grey).

Insertion into (7) yields

$$\dot{z}_i \;=\; f_i z_i \quad \text{and} \quad z_i(t) \;=\; z_i(0)\,\exp(f_i t)\;,$$

$$x_i(t) \;=\; x_i(0)\,\exp(f_i t)\,\exp\left(-\int_0^t \Phi(\tau)d\tau\right) \quad \text{with}$$

$$\exp\left(\int_0^t \Phi(\tau)d\tau\right) \;=\; \sum_{j=1}^{n} x_j(0)\,\exp(f_j t)\;,$$

where we have used $z_i(0) = x_i(0)$ and the condition $\sum_{i=1}^n x_i = 1$. The solution finally is of the form

$$x_i(t) \;=\; \frac{x_i(0)\,\exp(f_i t)}{\sum_{j=1}^n x_j(0)\,\exp(f_j t)}\;;\; i = 1, 2, \ldots, n\;. \tag{11}$$

Under the assumption that the largest fitness parameter is non-degenerate, $\max\{f_i;\, i = 1, 2, \ldots, n\} = f_m > f_i \,\forall\, i \neq m$, every solution curve fulfilling the initial condition $x_i(0) > 0$ approaches a homogenous population: $\lim_{t\to\infty} x_m(t) = \bar{x}_m = 1$ and $\lim_{t\to\infty} x_i(t) = \bar{x}_i = 0 \,\forall\, i \neq m$, and the flux approaches the largest fitness parameter monotonously, $\Phi(t) \to f_m$ (Examples are shown in figure 3).

Qualitative analysis of stationary points and their stability yields the following results:
(i) The only stationary points of equation (7) are the corners of the simplex, represented by the unit vectors $\mathbf{e}_k = \{x_k = 1, x_i = 0 \,\forall\, i \neq k\}$,
(ii) only one of these stationary points is asymptotically stable, the corner where the mean fitness Φ adopts its maximal value on the simplex ($\mathbf{e}_m$: $\bar{x}_m = 1$ defined by $\max\{f_i;\, i = 1, 2, \ldots, n\} = f_m > f_i \,\forall\, i \neq m$), one corner is unstable in all directions, a source where the value of Φ is minimal ($\mathbf{e}_s$: $\bar{x}_s = 1$ defined by $\min\{f_i;\, i = 1, 2, \ldots, n\} = f_s < f_i \,\forall\, i \neq s$), and all other $n - 2$ equilibria are saddle points, and
(iii) since $x_i(0) = 0$ implies $x_i(t) = 0 \,\forall\, t > 0$, every subsimplex of $\mathbb{S}_n^{(1)}$ is an invariant set, and thus the whole boundary of the simplex consists of invariant sets and subsets down the corners (which represent members of class $\mathbb{S}_1^{(1)}$).

3 Generalized gradient systems

Although $\Phi(t)$ represents a Liapunov-function for the dynamical system (7) and its existence is sufficient for the proof of global stability for *selection of the fittest* being the species with the largest f_k value, it is of interest that the differential equation (7) can be interpreted as a generalized gradient system [6–8] through the introduction of a Riemann-type metric based on a generalized scalar product defined at position $\mathbf{x}$

$$[\mathbf{u}, \mathbf{v}]_{(\mathbf{x})} \;=\; \sum_{i=1}^{n} \frac{u_i\, v_i}{x_i} \;.$$

In a gradient system,

$$\dot{x}_i \;=\; \frac{\partial V}{\partial x_i}(\mathbf{x})\,,\; i = 1, 2, \ldots, n \;\;\text{or}\;\; \dot{\mathbf{x}} \;=\; \nabla\, V(\mathbf{x}) \;, \tag{12}$$

the potential $V(\mathbf{x})$ increases steadily along the orbits,

$$\frac{dV}{dt} \;=\; \sum_{i=1}^{n} \left(\frac{\partial V}{\partial x_i}\,\frac{dx_i}{dt}\right) \;=\; \sum_{i=1}^{n} \left(\frac{\partial V}{\partial x_i}\right)^2 \;=\; \nabla\, V(\mathbf{x})\,,\; \nabla\, V(\mathbf{x}) \;\geq\; 0.$$

and it does so at a maximal rate, since the velocity vector, being equal to the gradient, points at the position of maximum increase of V. In other words,

the velocity vector points in the direction of steepest ascent, which is always orthogonal to the constant level sets of V. In gradient systems we observe optimization of the potential function $V(\mathbf{x})$ along all orbits.

For the purpose of illustration we choose an example, equation (12) with

$$V(\mathbf{x}) \;=\; -\frac{1}{2}\sum_{i=1}^{n} f_i x_i^2 \;\text{ and }\; \frac{dx_i}{dt} \;=\; \frac{\partial V}{\partial x_i}(\mathbf{x}) \;=\; -\,f_i x_i \;.$$

The time derivative of the potential function is obtained by

$$\frac{dV}{dt} \;=\; \sum_{i=1}^{n}\left(\frac{\partial V}{\partial x_i}\right)^2 \;=\; \sum_{i=1}^{n} f_i^2 x_i^2 \;\geq\; 0 \;.$$

The potential is increasing until it reaches asymptotically the maximal value $V = 0$. Solutions of the differential equation are computed by integration: $x_i(t) = x_i(0)\,\exp(-f_i t)\,\forall\, i = 1, \ldots, n$. The result derived from dV/dt is readily verified, since $\lim_{t\to\infty} x_i(t) = 0\,\forall\, i = 1, \ldots, n$ and hence $\lim_{t\to\infty} V(t) = 0$.

Equation (7), on the other hand, is not an ordinary gradient system: It fulfills the optimization criterion but the orbits are not orthogonal to the constant level sets of $V(\mathbf{x}) = \Phi(\mathbf{x})$ (see figure 3). In such a situation, it is often possible to achieve the full gradient properties through a generalization of the scalar product that is tantamount to a redefinition of the angle on the underlying space, $\mathbb{R}^n$ or $\mathbb{S}_n^{(1)}$, respectively. We shall describe here the formalism by means of the selection equation (7) as an example.

The potential function is understood as a map, $V(\mathbf{x}) :\; \mathbb{R}^n \Rightarrow \mathbb{R}^1$. The derivative of the potential $DV_{(\mathbf{x})}$ is the unique linear map $L :\; \mathbb{R}^n \Rightarrow \mathbb{R}^1$ that fulfils for all $\mathbf{y} \in \mathbb{R}^n$:

$$V(\mathbf{x}+\mathbf{y}) \;=\; L(\mathbf{y}) \,+\, o(\mathbf{y}) \;=\; DV_{(\mathbf{x})}(\mathbf{y}) \,+\, o(\mathbf{y}) \;,$$

where for $o(\mathbf{y})$ holds $o(\mathbf{y})/\|\mathbf{y}\| \to 0$ as $\|\mathbf{y}\| \to 0$. To L corresponds a uniquely defined vector $\mathbf{l} \in \mathbb{R}^n$ such that $\langle \mathbf{l}, \mathbf{y}\rangle = L(\mathbf{y})$ where $\langle *, *\rangle$ is the conventional Euclidean inner product defined by $\langle \mathbf{u}, \mathbf{v}\rangle = \sum_{i=1}^{n} u_i v_i$ for $\mathbf{u}, \mathbf{v} \in \mathbb{R}^n$. This special vector $\mathbf{l}$ is the gradient of the potential V, which can be defined therefore by the following mapping of $\mathbf{y}$ into $\mathbb{R}^1$:

$$\langle \operatorname{grad} V(\mathbf{x}), \mathbf{y}\rangle \;=\; DV_{(\mathbf{x})}(\mathbf{y}) \;\text{ for }\; \mathbf{y} \in \mathbb{R}^n \;. \tag{13}$$

The conventional Euclidean inner product is associated with the Euclidean metric, $\|\mathbf{x}\| = \langle \mathbf{x}, \mathbf{x}\rangle^{1/2}$.

It is verified straightforwardly that equation (7) does not fulfill the condition of a conventional gradient (13). The idea is now to replace the Euclidean metric by another more general metric that allows to recover the properties

of the gradient system. We introduce a generalized inner product corresponding to a Riemann-type metric where the conventional product terms are weighted by the coordinates of the position vector $\mathbf{z}$:

$$[\mathbf{u}, \mathbf{v}]_{\mathbf{z}} \;=\; \sum_{i=1}^{n} \frac{1}{z_i}\, u_i v_i \;. \tag{14}$$

Expression (14), $[*, *]_{\mathbf{z}}$, defines an inner product in the interior of $\mathbb{R}^n_+$, because it is linear in $\mathbf{u}$ and $\mathbf{v}$, and satisfies $[\mathbf{u}, \mathbf{u}]_{\mathbf{z}} \geq 0$ with the equality fulfilled if and only if $\|\mathbf{u}\| = 0$. Based on this choice of the inner product we redefine the gradient:

$$\big[\mathrm{Grad}[V(\mathbf{x})], \mathbf{y}\big]_{\mathbf{x}} \;=\; DV_{(\mathbf{x})}(\mathbf{y}) \;\; \text{for} \;\; \mathbf{x}, \mathbf{y} \in \mathbb{R}^n_+ \;. \tag{15}$$

The differential $DV_{(\mathbf{x})}$ is defined completely by $V(\mathbf{x})$ and hence independent of the choice of an inner product, the gradient, however, is not because it depends on the definition (15). Shahshahani [6] has shown that the relation $d\mathbf{x}/dt = \mathrm{Grad}\big[\Phi(\mathbf{x})\big]$ is fulfilled for Fisher's selection equation (19; see section 5) with $\Phi = \sum_{i=1}^{n} \sum_{j=1}^{n} a_{ij} x_i x_j$. As an example for the procedure we consider here the simple selection equation (7) with $\Phi = \sum_{i=1}^{n} f_i x_i$.

The differential equation (7) is conceived as a generalized gradient system and we find:

$$\frac{d\mathbf{x}}{dt} \;=\; \begin{pmatrix} x_1(f_1 - \sum_{j=1}^{n} f_j x_j) \\ x_2(f_2 - \sum_{j=1}^{n} f_j x_j) \\ \vdots \\ x_n(f_n - \sum_{j=1}^{n} f_j x_j) \end{pmatrix} \;=\; \mathrm{Grad}\big[V(\mathbf{x})\big] \;.$$

By application of equation (15) we obtain

$$DV_{(\mathbf{x})}(\mathbf{e}_i) \;=\; f_i \,-\, \sum_{j=1}^{n} f_j x_j \;,$$

which can be derived by conventional differentiation from

$$V(\mathbf{x}) \;=\; \sum_{i=1}^{n} x_i \left(2 f_i - \Phi\right) \;.$$

By straightforward computation we find the desired result:

$$V(\mathbf{x}) = \sum_{i=1}^{n} x_i \left(2 f_i - \Phi\right) = 2\Phi - \Phi = \Phi \;.$$

With the new definition of the scalar product, encapsulated in the definition of "Grad", the orbits of equation (7) are perpendicular to the constant level sets of $\Phi(\mathbf{x})$.

4 Complementary replication

Often the molecular mechanism of replication proceeds through an intermediate represented by a polynucleotide molecules with a complementary sequence: $(\mathbf{A}) + \mathbf{I}_+ \rightarrow \mathbf{I}_+ + \mathbf{I}_-$ and $(\mathbf{A}) + \mathbf{I}_- \rightarrow \mathbf{I}_- + \mathbf{I}_+$.In analogy to equation (7) and with $f_1 = \tilde{f}_+ [\mathbf{A}]$, $f_2 = \tilde{f}_- [\mathbf{A}]$, $x_1 = [\mathbf{I}_+]$, and $x_2 = [\mathbf{I}_-]$ we obtain the following differential equation [9–11]:

$$\begin{aligned} \dot{x_1} &= f_2 x_2 - x_1 \Phi \quad \text{and} \\ \dot{x_2} &= f_1 x_1 - x_2 \Phi \quad \text{with} \quad \Phi = f_1 x_1 + f_2 x_2 \; . \end{aligned} \tag{16}$$

Applying the integrating factor transformation (10) yields the linear equation

$$\dot{z_1} = f_2 z_2 \quad \text{and} \quad \dot{z_2} = f_1 z_1 \quad \text{or} \quad \dot{\mathbf{z}} = \mathrm{W} \cdot \mathbf{z} \, ; \; \mathbf{z} = \begin{pmatrix} z_1 \\ z_2 \end{pmatrix} , \; \mathrm{W} = \begin{pmatrix} 0 & f_2 \\ f_1 & 0 \end{pmatrix} .$$

The eigenvalues and (right hand) eigenvectors of the matrix W are

$$\begin{aligned} \lambda_{1,2} &= \pm\sqrt{f_1 f_2} \; = \pm f \quad \text{with} \quad f = \sqrt{f_1 f_2}, \\ \boldsymbol{\ell}_1 &= \begin{pmatrix} \sqrt{f_2} \\ \sqrt{f_1} \end{pmatrix} \quad \text{and} \quad \boldsymbol{\ell}_2 = \begin{pmatrix} -\sqrt{f_2} \\ \sqrt{f_1} \end{pmatrix} \; . \end{aligned} \tag{17}$$

Straightforward calculation yields analytical expressions for the two variables (see paragraph mutation) with the initial concentrations $x_1(0)$ and $x_2(0)$, and $\gamma_1(0) = \sqrt{f_1} x_1(0) + \sqrt{f_2} x_2(0)$ and $\gamma_2(0) = \sqrt{f_1} x_1(0) - \sqrt{f_2} x_2(0)$ as abbreviations:

$$\begin{aligned} x_1(t) &= \frac{\sqrt{f_2}\left(\gamma_1(0)\, e^{ft} + \gamma_2(0)\, e^{-ft}\right)}{(\sqrt{f_1} + \sqrt{f_2})\gamma_1(0)\, e^{ft} - (\sqrt{f_1} - \sqrt{f_2})\gamma_2(0)\, e^{-ft}} \\ x_2(t) &= \frac{\sqrt{f_1}\left(\gamma_1(0)\, e^{ft} - \gamma_2(0)\, e^{-ft}\right)}{(\sqrt{f_1} + \sqrt{f_2})\gamma_1(0)\, e^{ft} - (\sqrt{f_1} - \sqrt{f_2})\gamma_2(0)\, e^{-ft}} \; . \end{aligned} \tag{18}$$

After sufficiently long time the negative exponential has vanished and we obtain the simple result

$$x_1(t) \rightarrow \sqrt{f_2}/(\sqrt{f_1} + \sqrt{f_2}) \, , \; x_2(t) \rightarrow \sqrt{f_1}/(\sqrt{f_1} + \sqrt{f_2}) \;\; \text{as} \;\; \exp(-kt) \rightarrow 0 \, .$$

After an initial period, the plus-minus pair, $\mathbf{I}_\pm$, grows like a single autocatalyst with a fitness value $f = \sqrt{f_1 f_2}$ and a stationary ratio of the concentrations of complementary stands $x_1/x_2 \approx \sqrt{f_2}/\sqrt{f_1}$.

5 Recombination

Recombination of n alleles on a single locus is described by Ronald Fisher's [12] selection equation,

$$\begin{aligned} \dot{x}_i \;&=\; \sum_{j=1}^{n} a_{ij}x_ix_j \;-\; x_i\sum_{j=1}^{n}\sum_{k=1}^{n} a_{jk}x_jx_k \;=\; x_i(\sum_{j=1}^{n} a_{ij}x_j \;-\; \Phi) \\ &\text{with}\;\; \Phi = \sum_{j=1}^{n}\sum_{k=1}^{n} a_{jk}x_jx_k\,. \end{aligned} \tag{19}$$

As in the simple selection case the two conditions $a_{ij} > 0\,\forall\, i,j = 1,2,\ldots,n$ and $x_i \geq 0\,\forall\, i = 1,2,\ldots,n$ will guarantee $\Phi(t) \geq 0$. Summation of allele frequencies, $\sum_{i=1}^{n} x_i(t) = c(t)$, yields again equation (8) for $\dot{c}$ and hence, for $\sum_{i=1}^{n} x_i(0) = 1$ the population is confined again to the unit simplex.
The rate parameters a_{ij} form a quadratic matrix

$$\mathrm{A} \;=\; \begin{pmatrix} a_{11} & a_{12} & \ldots & a_{1n} \\ a_{21} & a_{22} & \ldots & a_{2n} \\ \vdots & \vdots & \ddots & \vdots \\ a_{n1} & a_{n2} & \ldots & a_{nn} \end{pmatrix}\,.$$

The dynamics of equation (19) for general matrices A may be very complicated [13]. In case of Fisher's selection equation, however, we are dealing with a symmetric matrix for biological reasons,[5] and then the differential equation can be subjected to straightforward qualitative analysis.

The introduction of mean rate parameters $\overline{a}_i = \sum_{j=1}^{n} a_{ij}x_j$ facilitates the forthcoming analysis. The time dependence of Φ is now given by

$$\begin{aligned} \frac{d\Phi}{dt} \;&=\; \sum_{i=1}^{n}\sum_{j=1}^{n} a_{ij}\left(\frac{dx_i}{dt}\,x_j \;+\; x_i\,\frac{dx_j}{dt}\right) \;=\; 2\sum_{i=1}^{n}\sum_{j=1}^{n} a_{ji}\,x_i\,\frac{dx_j}{dt} \;= \\ &=\; 2\sum_{i=1}^{n}\sum_{j=1}^{n} a_{ji}\,x_i\,\left(\sum_{k=1}^{n} a_{jk}x_jx_k \;-\; x_j\sum_{k=1}^{n}\sum_{\ell=1}^{n} a_{k\ell}x_kx_\ell\right) \;= \\ &=\; 2\sum_{j=1}^{n} x_j\sum_{i=1}^{n} a_{ji}x_i\sum_{k=1}^{n} a_{jk}x_k \;-\; 2\sum_{j=1}^{n} x_j\sum_{i=1}^{n} a_{ji}x_i\sum_{k=1}^{n} x_k\sum_{\ell=1}^{n} a_{k\ell}x_\ell \;= \\ &=\; 2\left(<\overline{a}^2> \;-\; <\overline{a}>^2\right) \;=\; 2\,\mathrm{var}\{\overline{a}\} \;\geq\; 0\,. \end{aligned} \tag{20}$$

[5]The assumption for Fisher's equation is based on insensitivity of phenotypes to the origin of the parental alleles on chromosomes. Phenotypes derived from genotype $\mathbf{a}_i\,\mathbf{a}_j$ are assumed to develop the same properties, no matter which allele, $\mathbf{a}_i$ or $\mathbf{a}_j$, on the chromosomal locus comes from the mother and which comes from the father. New results on genetic diseases have shown, however, that this assumption can be questioned.

Again we see that the flux $\Phi(t)$ is a non-deceasing function of time, and it approaches an optimal value on the simplex. This result is often called Fisher's fundamental theorem of evolution (see, e.g., [14]).

Qualitative analysis of equation (19) yields $2^n - 1$ stationary points, which depending on the elements of matrix A may lie in the interior, on the boundary or outside the unit simplex $\mathbb{S}_n^{(1)}$. In particular, we find at maximum one equilibrium point on the simplex and one on each subsimplex of the boundary. For example, each corner, represented by the unit vector $\mathbf{e}_k = \{\bar{x}_k = 1, x_i = 0 \,\forall\, i \neq k\}$, is a stable or unstable stationary point. In case there is an equilibrium in the interior of $\mathbb{S}_n^{(1)}$ it may be stable or unstable depending on the elements of A. In summary, this leads to a rich collection of different dynamical scenarios which share the absence of oscillations or chaotic dynamics. As said above, multiple stationary states do occur and more than one may be stable. This implies that the optimum, which $\Phi(t)$ is approaching, need not be uniquely defined. Instead $\Phi(t)$ may approach one of the local optima and then the outcome of the selection process will depend on initial conditions [14–17].

Three final remarks are important for a proper understanding of Fisher's fundamental theorem: (i) Selection in the one-locus system when it follows equation (19) optimizes mean fitness of the population, (ii) the outcome of the process need not be unique since the mean fitness Φ may have several local optima on the unit simplex, and (iii) optimization behavior that is susceptible to rigorous proof is restricted to the one locus model since systems with two or more gene loci may show different behavior of $\Phi(t)$.

6 Mutation

The introduction of mutation into the selection equation (7) based on knowledge from molecular biology is due to Manfred Eigen [9]. It leads to

$$\dot{x_i} \;=\; \sum_{j=1}^{n} Q_{ij}\, f_j\, x_j \;-\; x_i\, \Phi\,;\; i = 1, 2, \ldots, n \;\text{ with }\; \Phi = \sum_{j=1}^{n} f_j x_j = \overline{f}\;. \quad (21)$$

Mutations and error-free replication are understood as parallel reaction channels, the corresponding reaction probabilities are contained in the mutation matrix

$$\mathrm{Q} \;=\; \begin{pmatrix} Q_{11} & Q_{12} & \ldots & Q_{1n} \\ Q_{21} & Q_{22} & \ldots & Q_{2n} \\ \vdots & \vdots & \ddots & \vdots \\ Q_{n1} & Q_{n2} & \ldots & Q_{nn} \end{pmatrix} \;,$$

where Q_{ij} expresses the frequency of a mutation $\mathbf{I}_j \to \mathbf{I}_i$. Since the elements of Q are defined as reaction probabilities and a replication event yields either a correct copy or a mutant, the columns of Q sum up to one, $\sum_{i=1}^{n} Q_{ij} = 1$, and hence, Q is stochastic matrix. In case one makes the assumption of equal probabilities for $\mathbf{I}_j \to \mathbf{I}_i$ and $\mathbf{I}_i \to \mathbf{I}_j$, as it is made for example in the uniform error rate model (see equation (29) and [10,18]), Q is symmetric and hence, a bistochastic matrix.[6] The mean fitness or flux Φ is described by the same expression as in the selection-only case (7). This implies that the system converges to the unit simplex, as it did without mutations. For initial values of the variables chosen on the simplex, $\sum_{i=1}^{n} x_i(0) = 1$, it remains there.

In the replication-mutation system the boundary of the unit simplex, $\mathbb{S}_n^{(1)}$, is not invariant. Although no orbit starting on the simplex will leave it, which is a *conditio sine qua non* for chemical reactions requiring non-negative concentrations, trajectories flow from outside the positive orthant into $\mathbb{S}_n^{(1)}$. In other words, the condition $x_i(0) = 0$ does **not** lead to $x_i(t) = 0 \,\forall\, t > 0$. The chemical interpretation is straightforward: If a variant $\mathbf{I}_i$ is not present initially, it can, and depending on Q commonly will, be formed through a mutation event.

6.1 Exact solution

Before discussing the role of the flux Φ in the selection-mutation system, we shall derive exact solutions of equation (21) following a procedure suggested in [19,20]. At first the variables $x_i(t)$ are transformed as in the selection-only case (10):

$$z_i(t) \;=\; x_i(t)\, \exp\left(\int_0^t \Phi(\tau) d\tau\right) \;.$$

From $\sum_{x=1}^{n} x_i(t) = 1$ follows straightforwardly – again as in the selection-only case – the equation

$$\exp\left(\int_0^t \Phi(\tau) d\tau\right) \;=\; \left(\sum_{i=1}^{n} z_i(t)\right)^{-1} \;.$$

What remains to be solved is a linear first order differential equation

$$\dot{z}_i \;=\; \sum_{j=1}^{n} Q_{ij} f_j \; z_j \,;\; i = 1, 2, \ldots, n \;, \tag{22}$$

which is readily done by means of standard linear algebra. We define a matrix $\mathrm{W} = \{W_{ij} = Q_{ij}\, f_j\} = \mathrm{Q} \cdot \mathrm{F}$ where $\mathrm{F} = \{F_{ij} = f_i\, \delta_{ij}\}$ is a diagonal

[6] Symmetry in the direction of mutations is commonly not fulfilled in nature. It is introduced as a simplification, which facilitates the construction of computer models for equation (21). Moreover, the assumption of a symmetric mutation matrix Q is not essential for the analytic derivation of solutions.

matrix, and obtain the differential equation in matrix form, $\dot{\mathbf{z}} = \mathrm{W} \cdot \mathbf{z}$. Provided matrix W is diagonalizable, which will always be the case when the mutation matrix Q is based on real chemical reaction mechanisms, the variables $\mathbf{z}$ can be transformed linearly by means of an invertible $n \times n$ matrix $\mathrm{L} = \{\ell_{ij};\, i,j = 1,\ldots,n\}$ with $\mathrm{L}^{-1} = \{h_{ij};\, i,j = 1,\ldots,n\}$ being its inverse,

$$\mathbf{z}(t) \;=\; \mathrm{L} \cdot \boldsymbol{\zeta}(t) \;\text{ and }\; \boldsymbol{\zeta}(t) \;=\; \mathrm{L}^{-1} \cdot \mathbf{z}(t) \;,$$

such that $\mathrm{L}^{-1} \cdot \mathrm{W} \cdot \mathrm{L} = \Lambda$ is diagonal. The elements of Λ, λ_k, are the eigenvalues of the matrix W. The right-hand eigenvectors of W are given by the columns of L, $\boldsymbol{\ell}_j = (\ell_{i,j};\, i = 1,\ldots,n)$, and the left-hand eigenvectors by the rows of L^{-1}, $\mathbf{h}_k = (h_{k,i};\, i = 1,\ldots,n)$, respectively. These eigenvectors can be addressed as the *normal modes* of selection-mutation kinetics. For strictly positive off-diagonal elements of W, implying the same for Q which says nothing more than every mutation $\mathbf{I}_i \to \mathbf{I}_j$ is possible, although the probability might be extremely small, Perron-Frobenius theorem holds (see, for example, [21] and next paragraph) and we are dealing with a non-degenerate largest eigenvalue λ_0,

$$\lambda_0 \;>\; |\lambda_1| \;\geq\; |\lambda_2| \;\geq\; |\lambda_3| \;\geq\; \ldots \;\geq\; |\lambda_n| \;, \tag{23}$$

and a corresponding dominant eigenvector $\boldsymbol{\ell}_0$ with strictly positive components, $\ell_{i0} > 0 \,\forall\, i = 1,\ldots,n$.[7] In terms of components the differential equation in $\boldsymbol{\zeta}$ has the solutions

$$\zeta_k(t) \;=\; \zeta_k(0)\, \exp(\lambda_k\, t) \;. \tag{24}$$

Transformation back into the variables $\mathbf{z}$ yields

$$z_i(t) \;=\; \sum_{k=0}^{n-1} \ell_{ik}\, c_k(0)\, \exp(\lambda_k\, t) \;, \tag{25}$$

with the initial conditions encapsulated in the equation

$$c_k(0) \;=\; \sum_{i=1}^{n} h_{ki}\, z_i(0) \;=\; \sum_{i=1}^{n} h_{ki}\, x_i(0) \;. \tag{26}$$

From here we obtain eventually the solutions in the original variables x_i in analogy to equation (11)

$$\begin{aligned} x_i(t) \;&=\; \frac{\sum_{k=0}^{n-1} \ell_{ik}\, c_k(0)\, \exp(\lambda_k\, t)}{\sum_{j=1}^{n} \sum_{k=0}^{n-1} \ell_{jk}\, c_k(0)\, \exp(\lambda_k\, t)} \;= \\ &=\; \frac{\sum_{k=0}^{n-1} \ell_{ik} \sum_{i=1}^{n} h_{ki}\, x_i(0)\, \exp(\lambda_k\, t)}{\sum_{j=1}^{n} \sum_{k=0}^{n-1} \ell_{jk} \sum_{i=1}^{n} h_{ki}\, x_i(0)\, \exp(\lambda_k\, t)} \;. \end{aligned} \tag{27}$$

[7] We introduce here an asymmetry in numbering rows and columns in order to point at the special properties of the largest eigenvalue λ_0 and the dominant eigenvector $\boldsymbol{\ell}_0$.

6.2 Perron-Frobenius theorem

Perron-Frobenius theorem comes in two versions [21], which we shall now consider and apply to the selection-mutation problem. The stronger version provides a proof for six properties of the largest eigenvector of non-negative primitive matrices[8] T:

(i) The largest eigenvalue is real and positive, $\lambda_0 > 0$,

(ii) a strictly positive right eigenvector $\boldsymbol{\ell}_0$ and a strictly positive left eigenvector $\mathbf{h}_0$ are associated with λ_0,

(iii) $\lambda_0 > |\lambda_k|$ holds for all eigenvalues $\lambda_k \neq \lambda_0$,

(iv) the eigenvectors associated with λ_0 are unique up to constant factors,

(v) if $0 \leq \mathrm{B} \leq \mathrm{T}$ is fulfilled and β is an eigenvalue of B, then $|\beta| \leq \lambda_0$, and, moreover, $|\beta| = \lambda_0$ implies $\mathrm{B} = \mathrm{T}$,

(vi) λ_0 is a simple root of the characteristic equation of T.

The weaker version of the theorem holds for irreducible matrices[9] T. All the above given assertions hold except (iii) has to be replaced by the weaker statement

(iii) $\lambda_0 \geq |\lambda_k|$ holds for all eigenvalues $\lambda_k \neq \lambda_0$.

Irreducible cyclic matrices can be used straightforwardly as examples in order to demonstrate the existence of conjugate complex eigenvalues (An example is discussed below). Perron-Frobenius theorem, in its strict or weaker form, holds not only for strictly positive matrices $\mathrm{T} > 0$ but also for large classes of mutation or value matrices ($\mathrm{W} \equiv \mathrm{T}$ being a primitive or an irreducible non-negative matrix) with off-diagonal zero entries corresponding to zero mutation rates. The occurrence of a non-zero element $t_{ij}^{(m)}$ in T^m implies the existence of a mutation path $\mathbf{I}_j \rightarrow \mathbf{I}_k \rightarrow \ldots \rightarrow \mathbf{I}_l \rightarrow \mathbf{I}_i$ with non-zero mutation frequencies for every individual step. This condition is almost always fulfilled in real systems.

[8] A square non-negative matrix $\mathrm{T} = \{t_{ij}; i, j = 1, \ldots, n;\ t_{ij} \geq 0\}$ is called *primitive* if there exists a positive integer m such that T^m is strictly positive: $\mathrm{T}^m > 0$ which implies $\mathrm{T}^m = \{t_{ij}^{(m)}; i, j = 1, \ldots, n; t_{ij}^{(m)} > 0\}$.

[9] A square non-negative matrix $\mathrm{T} = \{t_{ij}; i, j = 1, \ldots, n; t_{ij} \geq 0\}$ is called *irreducible* if for every pair (i, j) of its index set there exists a positive integer $m_{ij} \equiv m(i, j)$ such that $t_{ij}^{m_{ij}} > 0$. An irreducible matrix is called *cyclic* with period d, if the period of (all) its indices satisfies $d > 1$, and it is said to be acyclic if $d = 1$.

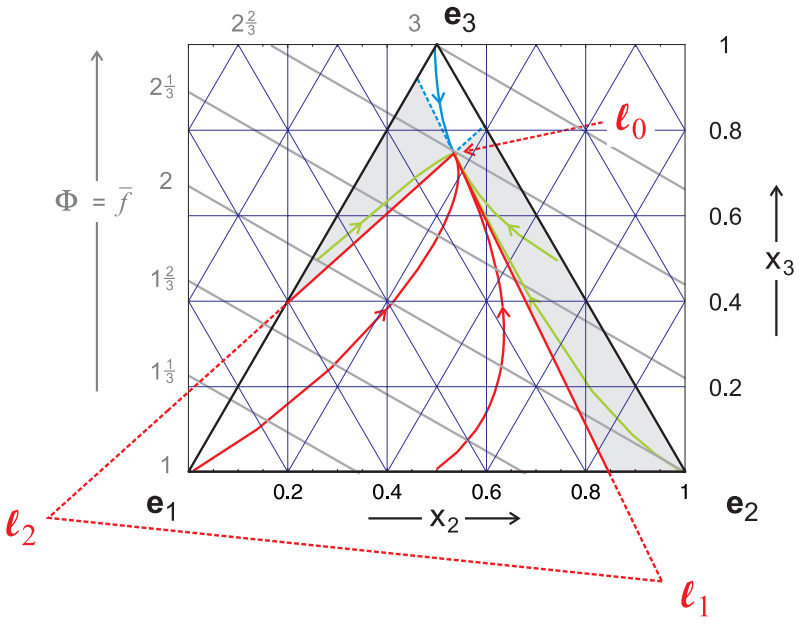

Figure 4: The quasispecies on the unit simplex. Shown is the case of three variables (x_1, x_2, x_3) on $\mathbb{S}_3^{(1)}$. The dominant eigenvector, the quasispecies denoted by $\boldsymbol{\ell}_0$, is shown together with the two other eigenvectors, $\boldsymbol{\ell}_1$ and $\boldsymbol{\ell}_2$. The simplex is partitioned into an *optimization cone* (white, red trajectories) where the mean replication rate $\bar{f}(t)$ is optimized, two other zones where $\bar{f}(t)$ may also decrease (grey), and the *master cone*, which is characterized by non-increasing $\bar{f}(t)$ and which contains the master sequence (white, blue trajectories). Here, $\mathbf{I}_3$ is chosen to be the master sequence. Solution curves are presented as parametric plots $\mathbf{x}(t)$. In particular, the parameter values are: $f_1 = 1.9\,[\mathrm{t}^{-1}]$, $f_2 = 2.0\,[\mathrm{t}^{-1}]$, and $f_3 = 2.1\,[\mathrm{t}^{-1}]$, the Q-matrix was assumed to be bistochastic with the elements $Q_{ii} = 0.98$ and $Q_{ij} = 0.01$ for $i, j = \{1, 2, 3\}$. Then the eigenvalues and eigenvectors of W are:

k	λ_k	ℓ_{1k}	ℓ_{2k}	ℓ_{3k}
0	2.065	0.093	0.165	0.742
1	1.958	0.170	1.078	-0.248
2	1.857	1.327	-0.224	-0.103

The mean replication rate $\bar{f}(t)$ is monotonously increasing along red trajectories, monotonously decreasing along the blue trajectory, and not necessarily monotonous along green trajectories. Constants level sets of Φ are straight lines (grey).

6.3 Complex eigenvalues

In order to address the existence of complex eigenvalues of the value matrix W we start by considering the straightforward case of a symmetric mutation matrix Q. Replication rate parameters, f_i are subsumed in a diagonal matrix: $\mathrm{F} = \{f_i\,\delta_{i,j}; i, j = 1, \ldots, n\}$, the value matrix is obtained as product $\mathrm{W} =$

$\mathrm{Q}\cdot\mathrm{F}$, and, in general, W is not symmetric. A similarity transformation,

$$\mathrm{F}^{\frac{1}{2}}\cdot\mathrm{W}\cdot\mathrm{F}^{-\frac{1}{2}} \;=\; \mathrm{F}^{\frac{1}{2}}\cdot\mathrm{Q}\cdot\mathrm{F}\cdot\mathrm{F}^{-\frac{1}{2}} \;=\; \mathrm{F}^{\frac{1}{2}}\cdot\mathrm{Q}\cdot\mathrm{F}^{\frac{1}{2}} \;=\; \mathrm{W}' \;.$$

yields a symmetric matrix [22], since $\mathrm{F}^{\frac{1}{2}}\cdot\mathrm{Q}\cdot\mathrm{F}^{\frac{1}{2}}$ is symmetric if Q is. Symmetric matrices have real eigenvalues and as a similarity transformation does not change the eigenvalues W has only real eigenvalues if Q is symmetric.

The simplest way to yield complex eigenvalues is introduction of cyclic symmetry into the matrix Q in such a way that the symmetry with respect to the main diagonal is destroyed. An example is the matrix

$$\mathrm{Q} \;=\; \begin{pmatrix} Q_{11} & Q_{12} & Q_{13} & \cdots & Q_{1n} \\ Q_{1n} & Q_{11} & Q_{12} & \cdots & Q_{1,n-1} \\ Q_{1,n-1} & Q_{1n} & Q_{11} & \cdots & Q_{1,n-2} \\ \vdots & \vdots & \vdots & \ddots & \vdots \\ Q_{12} & Q_{13} & Q_{14} & \cdots & Q_{11} \end{pmatrix} \;,$$

with different entries Q_{ij}. For equal replication parameters the eigenvalues contain complex n-th roots of one, $\gamma_k^n = 1$ or $\gamma_k = \exp(2\pi ik/n), i = 1,\ldots,n$, and for $n \geq 3$ most eigenvalues come in complex conjugate pairs. As mentioned earlier symmetry in mutation frequencies is commonly not fulfilled in nature. In case of point mutations the replacement of one particular base by another one does usually not occur with the same frequency as the inverse replacement, **G**→**A** versus **A**→**G** for example. Needless to stress, cyclic symmetry in mutation matrices is also highly improbable in real systems. The validity of Perron-Frobenius theorem, however, is not effected by the occurrence of complex conjugate pairs of eigenvectors. In addition, it is unimportant for most purposes whether a replication-mutation system approaches the stationary state monotonously or through damped oscillations (see next paragraph).

6.4 Mutation and optimization

In order to consider the optimization problem in the selection-mutation case, we choose the eigenvectors of W as the basis of a new coordinate system (figure 4):

$$\mathbf{x}(t) \;=\; \sum_{i=1}^{n} x_k(t)\,\mathbf{e}_i \;=\; \sum_{k=0}^{n-1} \xi_k(t)\,\boldsymbol{\ell}_k \;,$$

where the vectors $\mathbf{e}_i$ are the unit eigenvectors of the conventional Cartesian coordinate system and $\boldsymbol{\ell}_k$ the eigenvectors of W. The unit eigenvectors represent the corners of $\mathbb{S}_n^{(1)}$ and in complete analogy we denote the space defined

by the vectors $\boldsymbol{\ell}_k$ as $\tilde{\mathbb{S}}_n^{(1)}$. Formally, the transformed differential equation

$$\dot{\xi}_k \;=\; \xi_k\,(\lambda_k - \Phi)\,,\;\; k = 0, 1, \ldots, n-1 \;\;\text{with}\;\; \Phi = \sum_{k=0}^{n-1} \lambda_k \xi_k = \overline{\lambda}$$

is identical to equation (7) and hence the solutions are the same,

$$\xi_k(t) \;=\; \xi_k(0)\,\exp\left(\lambda_k\, t \;-\; \int_0^t \Phi(\tau)\,d\tau\right)\;,\;\; k = 0, 1, \ldots, n-1\;,$$

as well as the maximum principle **on** the simplex

$$\frac{d\Phi}{dt} \;=\; \sum_{k=0}^{n-1} \xi_k\;(\lambda_k - \Phi)^2 \;= <\lambda^2> \;-\; <\lambda>^2 \geq\; 0\;. \tag{9a}$$

The difference between selection and selection-mutation comes from the fact that the simplex $\tilde{\mathbb{S}}_n$ does not coincide with the physically defined space $\mathbb{S}_n$ (see figure 4 for a low-dimensional example). Indeed only the dominant eigenvector $\boldsymbol{\ell}_0$ lies in the interior of $\mathbb{S}_n^{(1)}$: It represent the stable stationary distribution of genotypes or **quasispecies** [10] towards which the solutions of the differential equation (21) converge. All other $n-1$ eigenvectors, $\boldsymbol{\ell}_1, \ldots, \boldsymbol{\ell}_{n-1}$ lie outside $\mathbb{S}_n^{(1)}$ in the *not physical* range where one or more variables x_i are negative. The quasispecies $\boldsymbol{\ell}_0$ is commonly dominated by a single genotype, called the **master sequence** $\mathbf{I}_m$, having the largest stationary relative concentration: $\bar{x}_m \gg \bar{x}_i \,\forall\, i \neq m$, reflecting, for not too large mutation rates, the same ranking as the elements of the matrix W: $W_{mm} \gg W_{ii} \,\forall\, i \neq m$. As sketched in figure 4 the quasispecies is then situated close to the unit vector $\mathbf{e}_m$ in the interior of $\mathbb{S}_n^{(1)}$.

For the discussion of the optimization behavior the simplex is partitioned into three zones: (i) The zone of maximization of $\Phi(t)$, the (large) lower white area in figure 4 where equation (9a) holds and which we shall denote as *optimization cone*,[10] (ii) the zone that includes the unit vector of the master sequence, $\mathbf{e}_m$, and the quasispecies, $\boldsymbol{\ell}_0$, as corners, and that we shall characterize as *master cone*,[10] and (iii) the remaining part of the simplex $\mathbb{S}_n^{(1)}$ (zones (iii) are colored grey in figure 4). It is straightforward to proof that increase of $\Phi(t)$ and monotonous convergence towards the quasispecies is restricted to the optimization cone [23]. From the properties of the selection equation (7) we recall and conclude that the boundaries of the simplex $\tilde{\mathbb{S}}_n^{(1)}$ are invariant sets. This implies that no orbit of the differential equation (21)

[10]The exact geometry of the optimization cone or the master cone is a polyhedron that can be approximated by a pyramid rather than a cone. Nevertheless we prefer the inexact notion *cone* because it is easier to memorize and to imagine in high-dimensional space.

can cross these boundaries. The boundaries of $\mathbb{S}_n^{(1)}$, on the other hand, are not invariant **but** they can be crossed exclusively in one direction: from outside to inside.[11] Therefore, a solution curve starting in the optimization cone or in the master cone will stay inside the cone where it started and eventually converge towards the quasispecies, $\boldsymbol{\ell}_0$.

In zone (ii), the master cone, all variables ξ_k except ξ_0 are negative and ξ_0 is larger than one in order to fulfill the $L^{(1)}$-norm condition $\sum_{k=0}^{n-1}\xi_k = 1$. In order to analyze the behavior of $\Phi(t)$ we split the variables into two groups, ξ_0 the frequency of the quasispecies and the rest [23], $\{\xi_k;\, k = 1,\ldots,n-1\}$ with $\sum_{k=1}^{n-1}\xi_k = 1-\xi_0$:

$$\frac{d\Phi}{dt} \;=\; \lambda_0\xi_0^2 \,+\, \sum_{k=1}^{n-1}\lambda_k^2\xi_k \,-\, \left(\lambda_0\xi_0 + \sum_{k=1}^{n-1}\lambda_k\xi_k\right)^2 \;.$$

Next we replace the distribution of λ_k values in the second group by a single λ-value, $\tilde{\lambda}$ and find:

$$\frac{d\Phi}{dt} \;=\; \lambda_0^2\xi_0 \,+\, \tilde{\lambda}^2(1-\xi_0) \,-\, \Big(\lambda_0\xi_0 + \tilde{\lambda}(1-\xi_0)\Big)^2 \;.$$

After a view simple algebraic operations we find eventually

$$\frac{d\Phi}{dt} \;=\; \xi_0\,(1-\xi_0)\,(\lambda_0 - \tilde{\lambda})^2 \;. \tag{28}$$

For the master cone with $\xi_0 \geq 1$, this implies $d\Phi(t)/dt \leq 0$, the flux is a non-increasing function of time. Since we are only interested in the sign of $d\Phi/dt$, the result is exact, because we could use the mean value $\tilde{\lambda} = \bar{\lambda} = (\sum_{k=1}^{n-1}\lambda_k\xi_k)/(1-\xi_0)$, the largest possible value λ_1 or the smallest possible value λ_{n-1} without changing the conclusion. Clearly, the distribution of λ_k-values matters for quantitative results. It is worth mentioning that equation (28) applies also to the quasispecies cone and gives the correct result that $\Phi(t)$ is non-decreasing. Decrease of mean fitness or flux $\Phi(t)$ in the master cone is readily illustrated: Consider, for example, a homogeneous population of the master sequence as initial condition: $x_m(0) = 1$ and $\Phi(0) = f_m$. The population becomes inhomogeneous because mutants are formed. Since all mutants have lower replication constants by definition, $(f_i < f_m\,\forall\, i \neq m)$, Φ becomes smaller. Finally, the distribution approaches the quasispecies $\boldsymbol{\ell}_0$ and $\lim_{t\to\infty}\Phi(t) = \lambda_0 < f_m$.

[11] This is shown easily by analyzing the differential equation, but follows also from the physical background: No acceptable process can lead to negative particle numbers or concentrations. It can, however, start at zero concentrations and this means the orbit begins at the boundary and goes into the interior of the physical concentration space, here the simplex $\mathbb{S}_n^{(1)}$.

An extension of the analysis from the master cone to zone (iii), where not all ξ_k values with $k \neq 0$ are negative, is not possible. It has been shown by means of numerical examples that $d\Phi(t)/dt$ may show non-monotonous behavior and can go through a maximum or a minimum at finite time [23].

6.5 Mutation rates and error threshold

In order to illustrate the influence of mutation rates on the selection process we apply (i) binary sequences, (ii) the uniform error rate approximation,

$$Q_{ij} \;=\; p^{\,d_{ij}}\,(1-p)^{\,\nu-d_{ij}} \tag{29}$$

with d_{ij} being the Hamming distance between the two sequences $\mathbf{I}_i$ and $\mathbf{I}_j$, ν the chain length and p the mutation or error rate per site and replication, and (iii) a simple model for the distribution of fitness values known as *single peak fitness landscape* [24],

$$f_1 \;=\; f_m \;>\; f_2 \;=\; f_3 \;=\; \ldots\; f_n \;=\; \bar{f}_{-m} \;=\; \frac{\sum_{i=2}^{n} f_i}{1-x_m}\;,$$

which represents a kind of mean field approximation. The mutants with the master sequence $\mathbf{I}_1$ are ordered in mutant classes: The zero-error class contains only the reference sequence ($\mathbf{I}_1$), the one-error class comprises all single point mutations, the two-error class all double point mutations, etc. Since the error rate p is independent of the particular sequence and all molecules belonging to the same mutant class have identical fitness values f_k, it is possible to introduce new variables for entire mutant classes Γ_k:

$$y_k \;=\; \sum_{j\,,\mathbf{I}_j\in\Gamma_k} x_j\;,\;\; k=0,1,\ldots,\nu\,,\;\sum_{k=0}^{\nu} y_k = 1\;. \tag{30}$$

The mutation matrix Q has to be adjusted to transitions between classes [24, 25]. For mutations from class Γ_l into Γ_k we calculate:

$$Q_{kl} \;=\; \sum_{i=l+k-\nu}^{\min(k,l)} \binom{k}{i}\binom{\nu-k}{l-i}\, p^{\,k+l-2i}(1-p)^{\,\nu-(k+l-2i)}\;. \tag{31}$$

The mutation matrix Q for error classes is not symmetric, $Q_{kl} \neq Q_{lk}$ as follows from equation (31).

A typical plot of relative concentrations against error rate is shown in figure 5. At vanishing error rates, $\lim p \to 0$, the master sequence is selected, $\lim_{t\to\infty} y_0(t) = \bar{y}_0 = 1$, and all other error classes vanish in the long time limit. Increasing error rates are reflected by a decrease in the stationary relative concentration of the master sequence and a corresponding increase

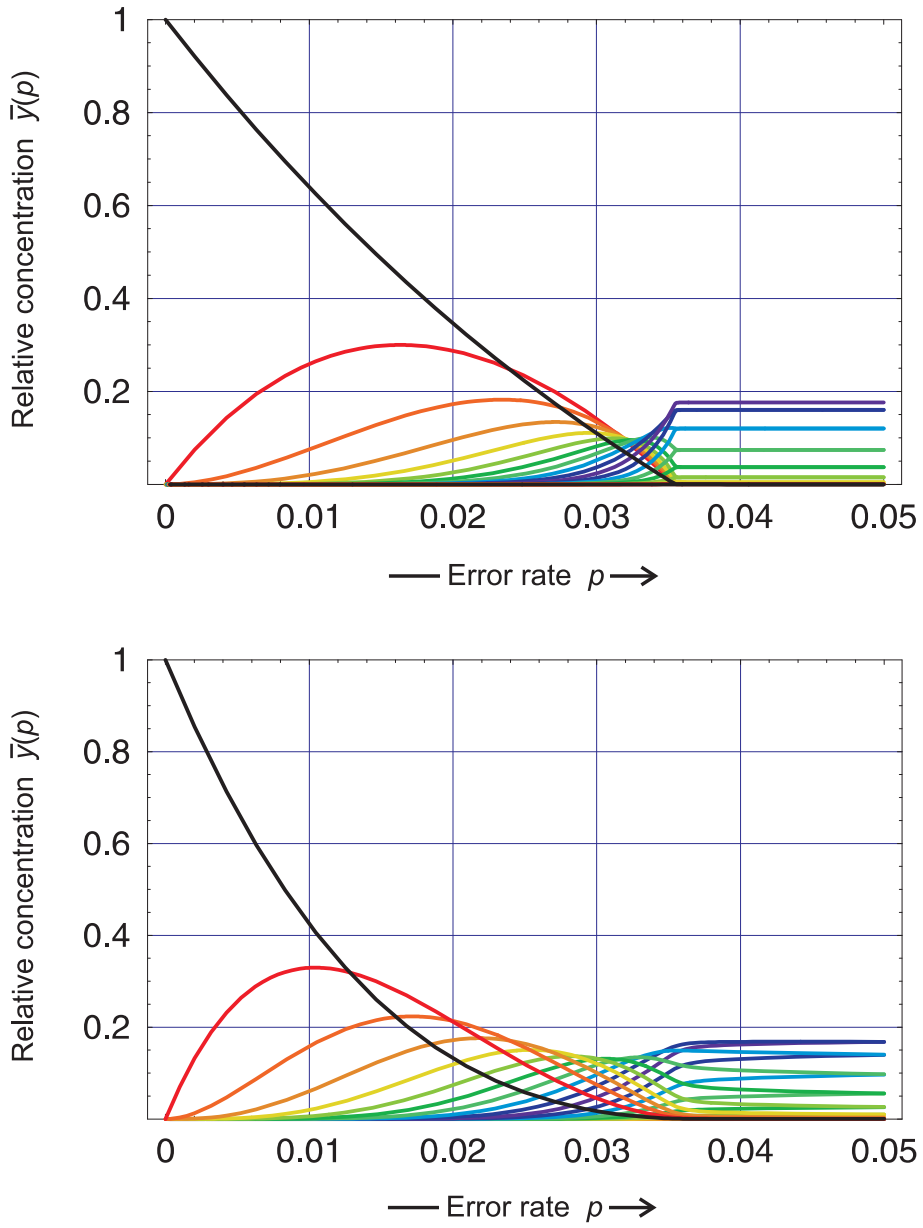

Figure 5: Error thresholds in the quasispecies model. The figures show the stationary distribution of relative concentrations of mutant classes as functions of the error rate, $\bar{y}_k(p)$, for sequences of chain length $\nu = 20$. The population on a *single peak landscape* (upper part, $\sigma = 2$) gives rise to a sharp transition between the ordered regime, where relative concentrations are determined by fitness values f_k and mutation rates Q_{kl} (31), and the domain of the uniform distribution where all error classes are present proportional to the numbers of sequences in them, $|\Gamma_k| = \binom{\nu}{k}$. The color code is chosen such that the error classes with the same frequency, for example Γ_0 and Γ_ν, Γ_1 and $\Gamma_{\nu-1}$, etc., have identical colors and hence, curves with the same color merge above threshold. The population on a *hyperbolic fitness landscape* (lower part, $\sigma = 1.905$) shows a smoother transition that can be characterized as *weak error threshold*. Careful observation shows that the coalescence of curves with different colors at $p \approx 0.05$ is accidental since they diverge again at higher error rates.

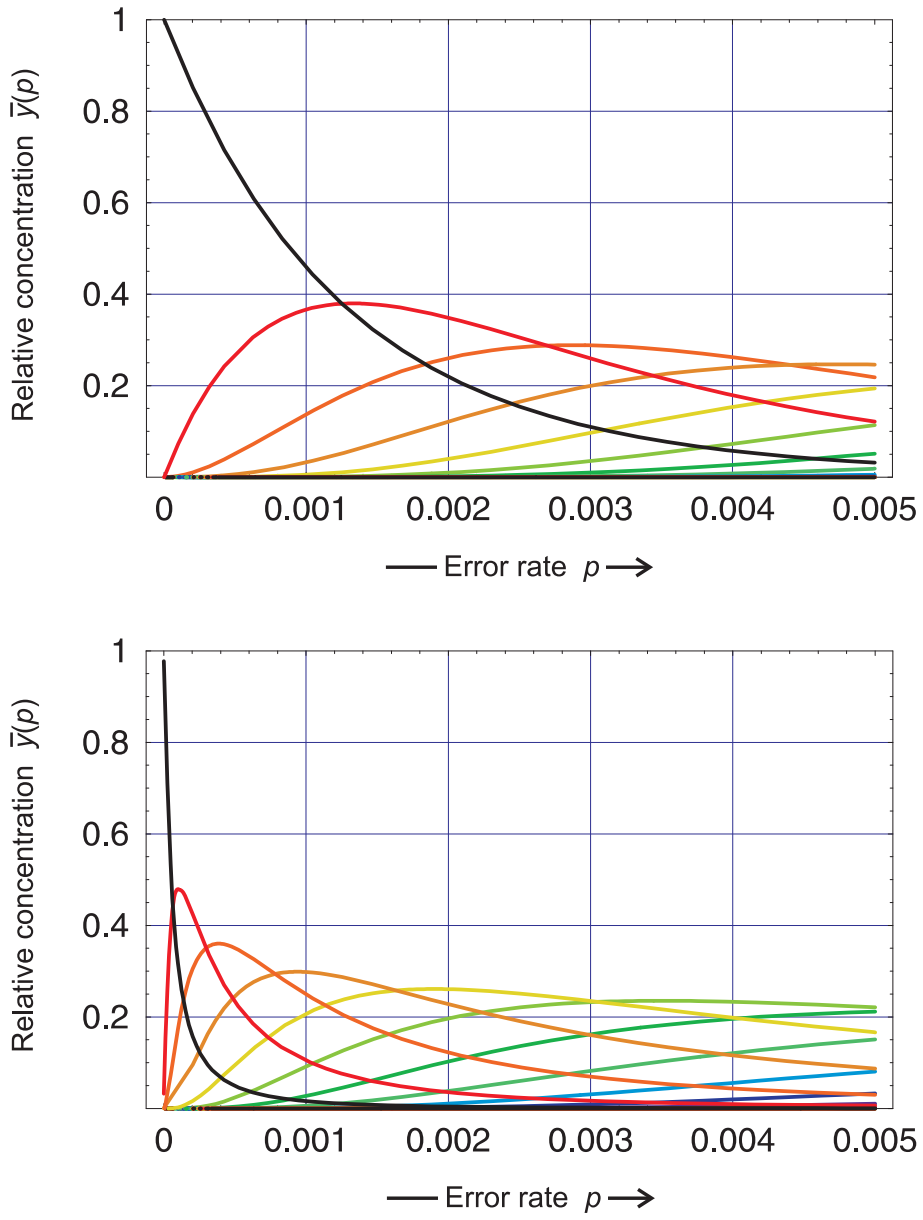

Figure 6: Smooth transitions in the quasispecies model. The two figures show stationary mutant distributions as functions of the error rate, $\bar{y}_k(p)$, for sequences of chain length $\nu = 20$. The upper figure was calculated for a *linear landscape* ($\sigma = 1.333$), the lower figure for a *quadratic landscape* ($\sigma = 1.151$) of fitness values. The transitions are smooth in both cases.

in the concentration of all mutant classes. Except $\bar{y}_0(p)$ all concentrations $\bar{y}_k(p)$ with $k < \nu/2$ go through a maximum and approach pairwise the curves for $\bar{y}_{\nu-k}$ at values of p that increase with p. At $p = 0.5$ the eigenvalue problem can be solved exactly: The largest eigenvalue is strictly positive $\lambda_0 > 0$, it corresponds to an eigenvector $\boldsymbol{\ell}_0$, which is the uniform distribution in relative stationary concentrations $\bar{x}_1 = \bar{x}_2 = \ldots = \bar{x}_n = 1/n$, and this implies $\bar{y}_k = \binom{\nu}{k}$ for the class variables. The uniform distribution is a result

of the fact that at $p = 0.5 = 1 - p$ correct digit replication and errors are equally probable (for binary sequences) and therefore we may characterize this scenario as *random replication*. All other eigenvalues vanish at $p = 0.5$: $\lambda_1 = \lambda_2 = \ldots = \lambda_{n-1} = 0$.

The mutant distribution $\bar{\mathbf{y}}(p)$ comes close to the uniform distribution already around $p \approx 0.035$ in figure 5, and stays constant for the rest of the p-values ($0.035 < p < 0.5$). The narrow transition from the *ordered replication* ($0 < p < 0.035$) to *random replication* ($p > 0.035$) is called the *error threshold*. An approximation based on neglect of mutational back-flow and using $\ln(1-p) \approx -p$ yields a simple expression for the position of the threshold [9]:

$$p_{\max} \;\approx\; \frac{\ln \sigma}{\nu} \quad \text{for small } p \; . \tag{32}$$

The equation defines a maximal error rate $p_{\max}$ above which no ordered – nonuniform – stationary distributions of sequences exist (see also section 7). In the current example (figure 5) we calculate $p_{\max} = 0.03466$ in excellent agreement with the value observed in computer simulations. RNA viruses commonly have mutation rates close to the error threshold [26]. Error rates can be increased by pharmaceutical drugs interfering with virus replication and accordingly, a new antiviral strategy has been developed, which drives virus replication into extinction either by passing the error threshold [27, 28] or by extinction. Recently, the mechanism of lethal mutagenesis in virus infections has been extensively discussed [29, 30].

Several model landscapes describing fitness by a monotonously decreasing function of the Hamming distance from the master sequence, $f(d)$, are often applied in population genetics, examples are:

$$\begin{aligned}
\text{hyperbolic}: \qquad f(d) &= f_0 - \frac{(f_0-1)(\nu+1)\,d}{\nu\,(d+1)}\,, \\
\text{linear}: \qquad f(d) &= f_0 - \frac{(f_0-1)\,d}{\nu}\,, \quad \text{and} \\
\text{quadratic}: \qquad f(d) &= f_0 - \frac{(f_0-1)\,d^2}{\nu^2}\;.
\end{aligned}$$

Interestingly, all three model landscapes do not sustain sharp error thresholds as observed with the single peak landscape. On the hyperbolic landscape the transition is less sharp than on the single peak landscape and may be called *weak error threshold*. The linear and the quadratic landscape show rather gradual and smooth transition from the quasispecies towards the uniform mutant distribution (Figure 6). Despite the popularity of smooth landscapes in populations genetics, they are not supported by knowledge derived form biopolymer structures and functions. In contrast, the available data provide

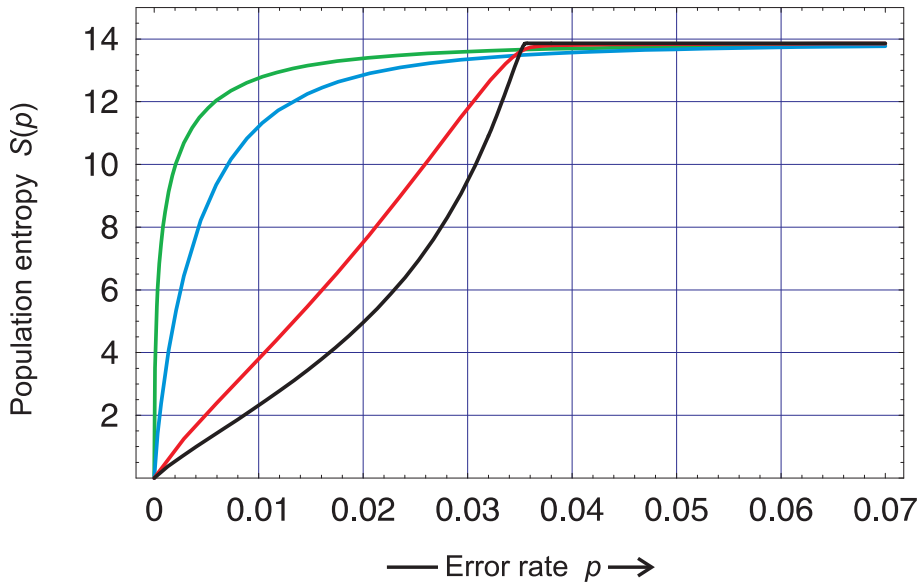

Figure 7: Population entropy on different fitness landscapes. The plot shows the population entropy as functions of the error rate, $S(p)$, for sequences of chain length $\nu = 20$. The results for individual landscapes are color coded: *single peak landscape* black, *hyperbolic landscape* red, *linear landscape* blue, and *quadratic landscape* green. The corresponding values for the superiority of the master sequence are: $\sigma = 2$, 1.905 , 1.333 , and 1.151 , respectively.

strong evidence that the natural landscapes are rugged and properties do not change gradually with Hamming distance.

In order to generalize the results derived from model landscapes to more realistic situations, random variations of rate constants for individual sequences were superimposed upon the fitness values of a single peak landscape – whereby the mean value $\bar{f}_{-m}$ was kept constant [31, pp.29-60]. Then, the curves for individual sequences within an error class differ from each other and form a band that increases in width with the amplitude of the random component. Interestingly, the error threshold phenomenon is retained thereby and the critical value $p_{\max}$ is shifted to lower error rates. Another very general approach to introduce variation into the value matrix without accounting for the underlying chemical reaction mechanism was taken by Walter Thirring and coworkers [32]. They also find a sharp transition between ordered and disordered domains.

6.6 Population entropies

Population entropies are suitable measures for the width of mutant distributions. For steady states they are readily computed from the largest eigen-

vector of matrix W:

$$S(p) \;=\; -\sum_{i=1}^{2^\nu} \bar{x}_i \,\ln\, \bar{x}_i \;=\; -\sum_{k=0}^{\nu} \bar{y}_k \left(\ln\, \bar{y}_k \,-\, \ln \binom{\nu}{k}\right) \;, \qquad (33)$$

where the expression on the r.h.s. refers to mutant classes. The pure state at $p = 0$ has zero entropy, $S(0) = 0$. For the uniform distribution the entropy is maximal, and for binary sequences we have,

$$S_{\max} \;=\; S(0.5) \;=\; \nu \,\ln\, 2 \;.$$

Between these two extremes, $0 \leq p \leq 0.5$, the entropy is a monotonously increasing function of the error rate, p. Figure 7 shows the entropy S(p) on the four model landscapes applied in figures 5 and 6. The curves reflect the threshold behavior encountered in the previous paragraphs (figures 5 and 5): the entropy on the single peak landscape makes a sharp kink at the position of the error threshold, the curve for the entropy on the hyperbolic landscape has a similar bend at the threshold but the transition is smoother, whereas the entropies for the two other landscapes are curved differently and approach smoothly the maximum value, $S_{\max} = \nu \,\ln\, 2$.

6.7 Lethal mutants

It is important to note that a quasispecies can exist also in cases where the Perron-Frobenius theorem is not fulfilled. As an example we consider an extreme case of lethal mutants: Only genotype $\mathbf{I}_1$ has a positive fitness value, $f_1 > 0$ and $f_2 = \ldots = f_n = 0$, and hence only the entries $W_{k1} = Q_{k1} f_1$ of matrix W are nonzero:

$$\mathrm{W} \;=\; \begin{pmatrix} W_{11} & 0 & \ldots & 0 \\ W_{21} & 0 & \ldots & 0 \\ \vdots & \vdots & \ddots & \vdots \\ W_{n1} & 0 & \ldots & 0 \end{pmatrix} \quad \text{and} \quad \mathrm{W}^k \;=\; W_{11}^k \begin{pmatrix} 1 & 0 & \ldots & 0 \\ \frac{W_{21}}{W_{11}} & 0 & \ldots & 0 \\ \vdots & \vdots & \ddots & \vdots \\ \frac{W_{n1}}{W_{11}} & 0 & \ldots & 0 \end{pmatrix} \;.$$

Accordingly, W is not primitive in this example, but under suitable conditions $\bar{\mathbf{x}} = (Q_{11}, Q_{21}, \ldots, Q_{n1})$ is a stable stationary mutant distribution and for $Q_{11} > Q_{j1} \,\forall\, j = 2, \ldots, n$ – correct replication occurs more frequently than a particular mutation – genotype $\mathbf{I}_1$ is the master sequence. On the basis of a rather idiosyncratic mutation model consisting in a one-dimensional chain of sequences the claim was raised that no quasispecies can be stable in presence of lethal mutants and accordingly, no error thresholds could exist [33]. Recent papers [30, 34], however, used a realistic high-dimensional mutation model and presented analytical results as well as numerically computed examples for error thresholds in the presence of lethal mutations.

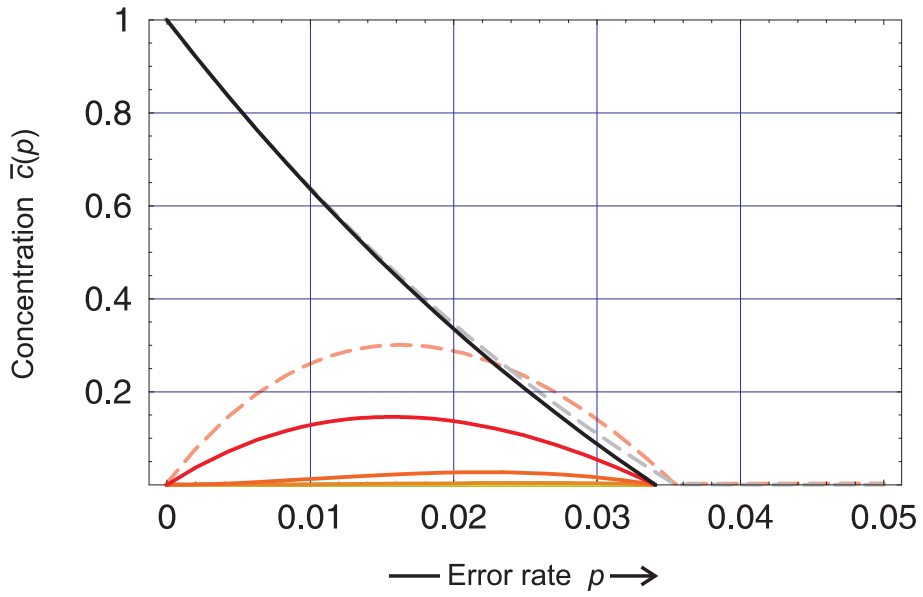

Figure 8: Lethal mutants and replication errors. The model for lethal mutants corresponding to a *single peak landscape* with $k_1 = 1$ and $k_2 = \ldots = k_n = 0$ is studied in the flowreactor. The concentrations of the master sequence (black) and the mutant classes (red, dark orange, light orange, etc.; full lines) are shown as functions of the error rate p. For the purpose of comparison the parameters were chosen with $\nu = 20$, $r = 1$, $a_0 = 2$, and $\eta = 2$. The plots are compared to the curves for the master sequence (grey; broken curve) and the one error class (light red; broken curve) in figure 5 (*single peak landscape* with $f_1 = 2$, $f_2 = \ldots = f_n = 1$, $\nu = 20$, and $\sigma = 2$.

In order to be able to handle the case of lethal mutants properly we have to go back to absolute concentrations in a realistic physical setup, the flowreactor applied in section 1 and shown in figure 1. We neglect degradation and find for $\mathbf{I}_1$ being the only viable genotype:[12]

$$\begin{aligned} \dot{a} &= -\left(\sum_{i=1}^{n} Q_{i1} k_1 c_1\right) a + r\,(a_0 - a) \\ \dot{c}_i &= Q_{i1} k_1 a c_1 - r c_i\,, \quad i = 1, 2, \ldots, n\,. \end{aligned} \tag{34}$$

Computation of stationary states is straightforward and yields two solutions, (i) the state of extinction with $\bar{a} = a_0$ and $\bar{c}_i = 0 \;\forall\; i = 1, 2, \ldots, n$, and (ii) a state of quasispecies selection consisting of $\mathbf{I}_1$ and its mutant cloud at the concentrations $\bar{a} = r/(Q_{11}k_1)$, $\bar{c}_1 = Q_{11}a_0 - r/k_1$, and $\bar{c}_i = \bar{c}_1(Q_{i1}/Q_{11})$ for $i = 2, \ldots, n$.

As an example we compute a maximum error rate for constant flow,

[12] We use k_i for the rate constants as in section 1, since $a(t)$ is a variable here.

$r = r_0$, again applying the uniform error rate model (29):

$$\begin{aligned} Q_{11} &= (1-p)^{\nu} \text{ and} \\ Q_{i1} &= p^{d_{i1}}\,(1-p)^{\nu-d_{i1}} \ , \end{aligned}$$

where d_{i1} again is the Hamming distance between the two sequences $\mathbf{I}_i$ and $\mathbf{I}_1$. Instead of the superiority σ of the master sequence – that diverges since $\bar{f}_{-m} = 0$ because of $f_2 = \ldots = f_n = 0$ – we use the dimensionless carrying capacity η, which can be defined to be

$$\eta \ = \ \frac{k_1\, a_0}{r_0}$$

for the flowreactor. The value of p, at which the stationary concentration of the master sequence $\bar{c}_1(p)$ and those of all other mutants vanishes, represents the analogue of the error threshold (32), and for the sake of clearness it is called the *extinction threshold*. Using $\ln(1-p) \approx -p$ again we obtain:

$$p_{\max} \ \approx \ \frac{\ln\,\eta}{\nu} \ \text{ for small } p \ . \tag{35}$$

The major difference between the error threshold (32) and the extinction threshold (35) concerns the state of the population at values $p > p_{\max}$: Replication with non-zero fitness of mutants leads to the uniform distribution, whereas the population goes extinct in the lethal mutant case. Accordingly, the transformation to relative concentrations fails and equation (7) is not applicable. In figure 8 we show an example for the extinction threshold with $\nu = 20$ and $\eta = 2$. For this case the extinction threshold is calculated from (35) to occur at $p_{\max} = 0.03466$ compared to a value of 0.03406 observed in computer simulations. In the figure we see also a comparison of the curves for the master sequence and the one error class for the single peak landscape and the lethality model. The agreement of the two curves for the master sequences is not surprise since the models were adjusted to coincide in the values $\bar{c}_1(0) = 1$ and $p_{\max} = \ln\,2/20$. The curves for the one error classes show some difference that is due to the lack of mutational backflow in case of lethal variants.

7 Limitations of the approach

An implicit assumption of the mathematical analysis of Darwinian selection presented here is the applicability of kinetic differential equations to describe selection and mutation in populations. In principle the approach by ordinary differential equations (ODEs) neglects finite size effects and hence is exact in principle for an infinite population size only. Biological populations, however,

may be small and low frequency mutants may be present often in a single copy or very few copies only. The uniform distribution at error rates above the threshold can never be achieved in reality because the numbers of possible polynucleotide sequences – 4^ν yielding, for example, 6×10^{45} sequences of tRNA length – are huge compared to typical populations ranging from 10^6 to 10^{15} individuals in replication experiments with bacteria, viruses, or RNA molecules. Typical situations in biology may thus differ drastically from scenarios in chemistry where large populations are distributed upon a few chemical species. Are the results derived from the differential equations then representative for real systems? Two situations can be distinguished: (i) Individual mutations are rare events and it is extremely unlikely that the same mutation occurs twice or is precisely reversed after it has occurred, and (ii) mutations are sufficiently frequent and occur in both directions within the time of observation. The second scenario is typical for virus evolution and *in vitro* evolution experiments with molecules. The first case seems to be fulfilled with higher organisms. Bacteria may be in an intermediate situation.

In scenario (i), i.e. at low mutation rates, the exact repetition of a given mutation is of very low probability. Back-mutations, precise inversions of mutations, are also of probability zero for all practical purposes. So-called compensatory mutations are known, but they are not back-mutations, they are rather caused by second mutations that compensate the effect of the first mutations. Then, a phenomenon called Muller's ratchet [35] in population genetics becomes effective in finite populations: Since lost mutants are not replaced, all variants starting with the fittest one will disappear sooner or later, and it is a only matter of time before a situation is reached where all genotypes have been replaced by others no matter what there fitness values were. For a comparison between the error threshold phenomenon and Muller's ratchet see [33].

The frequent mutation scenario (ii) allows for modeling and studying the kinetic equations of reproduction and selection as stochastic processes [25, 36–38] – examples are multitype branching or birth-and-death processes – as well as for computer simulations [39] (for an overview of stochastic modeling see, e.g., [40]). In essence, the solutions of stochastic models are time dependent probability distributions instead of solution curves. The mean or expectation value of the distribution coincides with the deterministic (ODE) solution, since all reactions in the kinetic model are (pseudo) first order. The relative width of the distribution increases with growing mutation rate and deceasing population size, and the error threshold phenomenon is reproduced as a superposition of error propagation and finite size effects. The expression

for the error threshold can be readily extended to finite populations [25]. Formation of stable quasispecies requires a replication fidelity that is the higher the smaller the population size is.

At error rates above threshold the kinetic ODEs predict the uniform distribution of sequences as stationary solution of equation (21).[13] Differences in fitness values do not matter under these conditions and there is no preferred master sequence. Realistic populations are by far too small to form uniform distributions of sequences and hence the deterministic model fails. Below threshold the quasispecies can be visualized as a localization of the population in some preferred region of sequence space with high fitness values (or at least one particularly high fitness value) [18, 41]. Above threshold the population is no more localized and drifts randomly in sequence space.[14] At the same time, populations are also too small to occupy a coherent region in sequence space and break up into smaller clones, which migrate in different directions as described for the neutral evolution case [3, 44].

How relevant is the error threshold in realistic situations? According to the results presented in section 6.5 the question boils down to an exploration of natural fitness landscapes: Are biopolymer landscapes rugged or smooth? All evidence obtained so far points towards a rather bizarre structures of these landscapes. Single nucleotide exchanges may lead to large effects, small effects or no consequences at all as in the case of neutral mutations. Since biomolecules are usually optimized with respect to their functions within an organism, most mutations have deleterious effects or no effect. Biopolymer landscapes have three characteristic features, which are hard to visualize: (i) high dimensionality, (ii) ruggedness, and (iii) neutrality. In case equally fit genotypes are nearest or next nearest neighbors in sequence space they form joint quasispecies as described in [23]. When they are not closely related, however, neutral evolution in the sense of Motoo Kimura is observed [45]. In case of neutrality in genotype space a selection model can still be formulated in phenotype space [46, 47]. The variables are concentrations of phenotypes that are obtained through lumping together all concentrations of genotypes, which form the same phenotype. Then, an analysis similar to the one presented here can be carried out. The genotypic error threshold is relaxed and

[13] As mentioned before the uniform distribution is the exact stationary solution of equation (21) for equal probabilities of correct and incorrect incorporation of a nucleotide, which is the case at an error rate $p = 1 - p = 0.5$ for binary sequences.

[14] The mutation rate can be seen as an analogue to temperature in spin systems and the error threshold corresponds to a phase transitions. The relation between the selection-mutation equation and spin systems has been studied first by Ira Leuthäusser [42, 43].

the system gives rise to a phenotypic error threshold below which the fittest or master phenotype is conserved in the population. The ODE model is readily supplemented by a theory of phenotype evolution based on new concept of evolutionary nearness of phenotypes in sequence space [4, 48, 49], which is confirmed by computer simulations of RNA structure optimization in a flowreactor of the type shown in figure 1 [4,48,50]. The article [50] deals also with random drift of populations on neutral subspaces of sequence space. A series of snapshots shows the spreading of a population that breaks up into individual clones in full agreement with earlier models [44, 51]. Computer simulations were also successful in providing evidence for the occurrence of error thresholds in stochastic replication-mutation systems [52].

References

[1] A. Watts and G. Schwarz, editors. *Evolutionary Biotechnology – From Theory to Experiment*, volume 66/2-3 of *Biophysical Chemistry*, pages 67–284. Elesvier, Amsterdam, 1997.

[2] W. Fontana and P. Schuster. A computer model of evolutionary optimization. *Biophys. Chem.*, 26:123–147, 1987.

[3] M. A. Huynen, P. F. Stadler, and W. Fontana. Smoothness within ruggedness. The role of neutrality in adaptation. *Proc. Natl. Acad. Sci. USA*, 93:397–401, 1996.

[4] W. Fontana and P. Schuster. Continuity in evolution. On the nature of transitions. *Science*, 280:1451–1455, 1998.

[5] D. Zwillinger. *Handbook of Differential Equations*. Academic Press, San Diego, CA, third edition, 1998.

[6] S. Shahshahani. A new mathematical framework for the study of linkage and selection. *Mem. Am. Math. Soc.*, 211, 1979.

[7] K. Sigmund. The maximum principle for replicator equations. In W. Ebeling and M. Peschel, editors, *Lotka-Volterra Approach to Cooperation and Competition in Dynamical Systems*, pages 63–71. Akademie-Verlag, Berlin, 1985.

[8] P. Schuster and K. Sigmund. Dynamics of evolutionary optimization. *Ber. Bunsenges. Phys. Chem.*, 89:668–682, 1985.

[9] M. Eigen. Selforganization of matter and the evolution of biological macromolecules. *Naturwissenschaften*, 58:465–523, 1971.

[10] M. Eigen and P. Schuster. The hypercycle. A principle of natural self-organization. Part A: Emergence of the hypercycle. *Naturwissenschaften*, 64:541–565, 1977.

[11] M. Eigen and P. Schuster. The hypercycle. A principle of natural self-organization. Part B: The abstract hypercycle. *Naturwissenschaften*, 65:7–41, 1978.

[12] R. A. Fisher. *The Genetical Theory of Natural Selection*. Oxford University Press, Oxford, UK, 1930.

[13] P. Schuster and K. Sigmund. Replicator dynamics. *J. Theor. Biol.*, 100:533–538, 1983.

[14] W. J. Ewens. *Mathematical Population Genetics*, volume 9 of *Biomathematics Texts*. Springer-Verlag, Berlin, 1979.

[15] E. Akin. *The Geometry of Population Genetics*, volume 31 of *Lecture Notes in Biomathematics*. Springer-Verlag, Berlin, 1979.

[16] J. Hofbauer and K. Sigmund. *Dynamical Systems and the Theory of Evolution*. Cambridge University Press, Cambridge, UK, 1988.

[17] P. Schuster. Potential functions and molecular evolution. In M. Markus, S. C. Müller, and G. Nicolis, editors, *From Chemical to Biological Organization. Springer Series in Synergetics*, volume 39, pages 149–165. Springer-Verlag, Berlin, 1988.

[18] M. Eigen, J. McCaskill, and P. Schuster. The molecular quasispecies. *Adv. Chem. Phys.*, 75:149–263, 1989.

[19] C. J. Thompson and J. L. McBride. On Eigen's theory of the self-organization of matter and the evolution of biological macromolecules. *Math. Biosci.*, 21:127–142, 1974.

[20] B. L. Jones, R. H. Enns, and S. S. Rangnekar. On the theory of selection of coupled macromolecular systems. *Bull. Math. Biol.*, 38:15–28, 1976.

[21] E. Seneta. *Non-negative Matrices and Markov Chains*. Springer-Verlag, New York, second edition, 1981.

[22] D. S. Rumschitzki. Spectral properties of Eigen evolution matrices. *J. Math. Biol.*, 24:667–680, 1987.

[23] P. Schuster and J. Swetina. Stationary mutant distribution and evolutionary optimization. *Bull. Math. Biol.*, 50:635–660, 1988.

[24] J. Swetina and P. Schuster. Self-replication with errors - A model for polynucleotide replication. *Biophys. Chem.*, 16:329–345, 1982.

[25] M. Nowak and P. Schuster. Error thresholds of replication in finite populations. Mutation frequencies and the onset of Muller's ratchet. *J. Theor. Biol.*, 137:375–395, 1989.

[26] J. W. Drake. Rates of spontaneous mutation among RNA viruses. *Proc. Natl. Acad. Sci. USA*, 90:4171–4175, 1993.

[27] M. Eigen. Error catastrophe and antiviral strategy. *Proc. Natl. Acad. Sci. USA*, 99:13374–13376, 2002.

[28] E. Domingo, ed. Virus entry into error catastrophe as a new antiviral strategy. *Virus Research*, 107(2):115–228, 2005.

[29] J. J. Bull, R. Sanjuan, and C. O. Wilke. Theory for lethal mutagenesis for viruses. *J. Virology*, 81:2930–2939, 2007.

[30] H. Tejero, A. Marín, and F. Montero. Effect of lethality on the extinction and on the error threshold of quasispecies. *J. Theor. Biol.*, 262:733–741, 2010.

[31] P. E. Phillipson and P. Schuster. *Modeling by Nonlinear Differential Equations. Dissipative and Conservative Processes*, volume 69 of *World Scientific Series on Nonlinear Science A*. World Scientific, Singapore, 2009.

[32] C. Marx, H. A. Posch, and W. Thirring. Emergence of order in selection-mutation dynamics. *Phys. Rev. E*, 75:061109, 2007.

[33] G. P. Wagner and P. Krall. What is the difference between models of error thresholds and Muller's ratchet. *J. Math. Biol.*, 32:33–44, 1993.

[34] N. Takeuchi and P. Hogeweg. Error-thresholds exist in fitness landscapes with lethal mutants. *BMC Evolutionary Biology*, 7: e15, 2007.

[35] H. J. Muller. Some genetic aspects of sex. *American Naturalist*, 66:118–138, 1932.

[36] P. Schuster and K. Sigmund. Random selection - A simple model based on linear birth and death processes. *Bull. Math. Biol.*, 46:11–17, 1984.

[37] J. S. McCaskill. A stochastic theory of macromolecular evolution. *Biol. Cybern.*, 50:63–73, 1984.

[38] L. Demetrius, P. Schuster, and K. Sigmund. Polynucleotide evolution and branching processes. *Bull. Math. Biol.*, 47:239–262, 1985.

[39] D. T. Gillespie. Stochastic simulation of chemical kinetics. *Annu. Rev. Phys. Chem.*, 58:35–55, 2007.

[40] R. A. Blythe and A. McKane. Stochastic models of evolution in genetice, ecology and linguistics. *J. Stat. Mech.: Theor. Exp.*, page P07018, 2007.

[41] J. S. McCaskill. A localization threshold for macromolecular quasispecies from continuously distributed replication rates. *J. Chem. Phys.*, 80:5194–5202, 1984.

[42] I. Leuthäusser. An exact correspondence between Eigen's evolution model and a two-dimensional ising system. *J. Chem. Phys.*, 84:1884–1885, 1986.

[43] I. Leuthäusser. Statistical mechanics of Eigen's evolution model. *J. Stat. Phys.*, 48:343–360, 1987.

[44] B. Derrida and L. Peliti. Evolution in a flat fittness landscape. *Bull. Math. Biol.*, 53:355–382, 1991.

[45] M. Kimura. *The Neutral Theory of Molecular Evolution*. Cambridge University Press, Cambridge, UK, 1983.

[46] C. Reidys, C. Forst, and P. Schuster. Replication and mutation on neutral networks. *Bull. Math. Biol.*, 63:57–94, 2001.

[47] N. Takeuchi, P. H. Poorthuis, and P. Hogeweg. Phenotypic error threshold – Additivity and epistasis in RNA evolution. *BMC Evolutionary Biology*, 5: e9, 2005.

[48] W. Fontana and P. Schuster. Shaping space. The possible and the attainable in RNA genotype-phenotype mapping. *J.Theor.Biol.*, 194:491–515, 1998.

[49] B. R. M. Stadler, P. F. Stadler, G. P. Wagner, and W. Fontana. The topology of the possible: Formal spaces underlying patterns of evolutionary change. *J. Theor. Biol.*, 213:241–274, 2001.

[50] P. Schuster. Molecular insight into the evolution of phenotypes. In J. P. Crutchfield and P. Schuster, editors, *Evolutionary Dynamics – Exploring the Interplay of Accident, Selection, Neutrality, and Function*, pages 163–215. Oxford University Press, New York, 2003.

[51] P. G. Higgs and B. Derrida. Stochastic models for species formation in evolving populations. *J. Phys. A: Math. Gen.*, 24:L985–L991, 1991.

[52] A. Kupczok and P. Dittrich. Determinants of simulated RNA evolution. *J. Theor. Biol.*, 238:726–735, 2006.

Notation

building blocks and degradation products	$\mathsf{A}, \mathsf{B}, \ldots,$
numbers of particles of $\mathsf{A}, \mathsf{B}, \ldots,$	$N_{\mathsf{A}}, N_{\mathsf{B}}, \ldots,$
concentrations of $\mathsf{A}, \mathsf{B}, \ldots,$	$[\mathsf{A}] = a, [\mathsf{B}] = b, \ldots,$
replicating molecular species	$\mathbf{I}_1, \mathbf{I}_2, \ldots,$
numbers of particles of $\mathbf{I}_1, \mathbf{I}_2, \ldots,$	$N_1, N_2, \ldots,$
concentrations of $\mathbf{I}_1, \mathbf{I}_2, \ldots,$	$[\mathbf{I}_1] = c_1, [\mathbf{I}_2] = c_2, \ldots,$
relative concentrations of $\mathbf{I}_1, \mathbf{I}_2, \ldots,$	$[\mathbf{I}_1] = x_1, [\mathbf{I}_2] = x_2, \ldots,$
partial sums of relative concentrations	$y_k = \sum_i x_i \,,$
flow rate into the CSTR	$r \,,$
influx concentration into the CSTR	$a_0 \,,$
mean residence time of a volume element in the CSTR	$\tau_r = r^{-1} \,,$
rate parameters	$d_i, k_i, f_i, \ldots \quad i = 1, 2, \ldots,$
global regulation flux	$\Phi(t) \,,$
chain length of polynucleotides	$\nu \,,$
superiority of the master sequence $\mathbf{I}_m$	$\sigma_m = \frac{f_m (1 - x_m)}{\sum_{i \neq m} f_i} \,,$
population entropy	$S = \sum_i x_i \ln x_i \,.$